NeuroImage 256 (2022) 119245

Contents lists available at ScienceDirect

NeuroImage

journal homepage: www.elsevier.com/locate/neuroimage

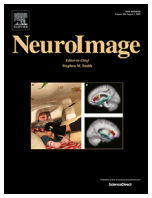

Variability and task-responsiveness of electrophysiological dynamics: Scale-free stability and oscillatory flexibility

Soren Wainio-Theberge[a,b,*], Annemarie Wolff[a], Javier Gomez-Pilar[c,d], Jianfeng Zhang[e,f], Georg Northoff[a,e,g,*]

[a] Mind, Brain Imaging, and Neuroethics Unit, Institute of Mental Health Research, Royal Ottawa Mental Health Centre, University of Ottawa, 1145 Carling Avenue, Rm. 6435, Ottawa, ON K1Z 7K4, Canada
[b] Integrated Program in Neuroscience, McGill University, Montréal, QC, Canada
[c] Biomedical Engineering Group, University of Valladolid, Paseo de Belén, 15, Valladolid 47011, Spain
[d] Centro de Investigación Biomédica en Red en Bioingeniería, Biomateriales y Nanomedicina, (CIBER-BBN), Valladolid, Spain
[e] Mental Health Centre/7th Hospital, Zhejiang University School of Medicine, Tianmu Road 305, Hangzhou, Zhejiang 310013, China
[f] College of Biomedical Engineering and Instrument Sciences, Zhejiang University, Hangzhou, China
[g] Centre for Cognition and Brain Disorders, Hangzhou Normal University, Hangzhou, Zhejiang 311121, China

ARTICLE INFO

Keywords:
Scale-free activity
Cortical oscillations
Neural variability
Stability
Flexibility
MEG

ABSTRACT

Cortical oscillations and scale-free neural activity are thought to influence a variety of cognitive functions, but their differential relationships to neural stability and flexibility has never been investigated. Based on the existing literature, we hypothesize that scale-free and oscillatory processes in the brain exhibit different trade-offs between stability and flexibility; specifically, cortical oscillations may reflect variable, task-responsive aspects of brain activity, while scale-free activity is proposed to reflect a more stable and task-unresponsive aspect. We test this hypothesis using data from two large-scale MEG studies (HCP: n = 89; CamCAN: n = 195), operationalizing stability and flexibility by task-responsiveness and spontaneous intra-subject variability in resting state. We demonstrate that the power-law exponent of scale-free activity is a highly stable parameter, which responds little to external cognitive demands and shows minimal spontaneous fluctuations over time. In contrast, oscillatory power, particularly in the alpha range (8–13 Hz), responds strongly to tasks and exhibits comparatively large spontaneous fluctuations over time. In sum, our data support differential roles for oscillatory and scale-free activity in the brain with respect to neural stability and flexibility. This result carries implications for criticality-based theories of scale-free activity, state-trait models of variability, and homeostatic views of the brain with regulated variables vs. effectors.

1. Introduction

Electrophysiological recordings of brain activity reveal two main types of neural dynamics: rhythmic cortical oscillations, and arrhythmic activity which follows a scale-free or power-law distribution (Donoghue et al., 2020; He, 2014). Cortical oscillations concern band-limited fluctuations in frequency ranges such as alpha (8–13 Hz), beta (13–30 Hz), or theta (4–8 Hz), which have been associated with various cellular processes and cognitive/behavioural domains (Buzsáki, 2006; Klimesch, 2012; Pfurtscheller and Lopes da Silva, 1999), and are modulated by a variety of different experimental tasks (Klimesch, 2012; Knyazev, 2007; Makeig, 1993). Arrhythmic activity, in contrast, refers to "scale-free" or "fractal" activity reflecting its characteristic $1/f^{\beta}$ distribution of power over frequencies; power decreases linearly on a log-log scale with increasing frequency such that the power spectrum has the same structure in multiple frequency ranges, giving the distribution its "scale-free" moniker. Scale-free brain activity has been less well studied than cortical oscillations, though it is of growing importance in electrophysiological studies (Donoghue et al., 2020; Eke et al., 2002; He, 2014; Linkenkaer-Hansen et al., 2001).

Scale-free processes are distinct in their generating physiological mechanisms (Lombardi et al., 2017; Pfurtscheller and Lopes da Silva, 1999; Poil et al., 2012) and neurovascular coupling (Wen and Liu, 2016a); for example, scale-free processes are associated with excitation-inhibition balance (Lombardi et al., 2017), and are more strongly related to the global fMRI signal than cortical oscillations (Wen and Liu, 2016a). Importantly, they are also related to cognitive

* Corresponding authors at: Mind, Brain Imaging, and Neuroethics Unit, Institute of Mental Health Research, Royal Ottawa Mental Health Centre, University of Ottawa, 1145 Carling Avenue, Rm. 6435, Ottawa, ON K1Z 7K4, Canada.
E-mail addresses: swain083@uottawa.ca (S. Wainio-Theberge), georg.northoff@theroyal.ca (G. Northoff).

https://doi.org/10.1016/j.neuroimage.2022.119245.
Received 24 June 2021; Received in revised form 17 April 2022; Accepted 22 April 2022
Available online 25 April 2022.

and clinical phenomena such as schizophrenia (Northoff et al., 2020; Sun et al., 2014), the self (Huang et al., 2016; Kolvoort et al., 2020; Wolff et al., 2018), consciousness (Tagliazucchi et al., 2016, 2013; Zhang et al., 2018; Zilio et al., 2020), and age-related cognitive decline (Dave et al., 2018; Voytek et al., 2015). However, cortical oscillations are also frequently implicated in similar cognitive processes (e.g. alpha and the self (Bai et al., 2016), or gamma band activity in schizophrenia (Williams and Boksa, 2010)), and few studies have compared scale-free activity with cortical oscillations to determine their different properties in rest and task states. Here, we present evidence that scale-free activity and cortical oscillations indeed take on different roles reflecting "stable" and "flexible" aspects of neural activity, respectively, with cortical oscillations displaying greater changes in both intra-subject variability and task-responsiveness than scale-free activity.

Behaviourally, flexibility refers to the ability to respond adaptively to environmental circumstances (for example, putting aside one's work and tending to a baby when it starts crying). Stability refers to the opposite end of this continuum, reflecting the preservation of certain attributes of behaviour despite competing stimuli (for example, focusing on one's writing despite the TV being on in the background). Behavioural flexibility has obvious desirable characteristics, and is often discussed in the context of set-shifting paradigms (Dajani and Uddin, 2015), the ability to modulate one's cognitive state (Garrett et al., 2013, 2011), or the ability to respond to unexpected stimuli that require attention (Goschke, 2003). However, in many cases behavioural stability is also desirable, such as when one must inhibit distraction and focus on a goal (Dreisbach et al., 2005; Goschke, 2003), or in order to maintain a generalizable internal working model of the environment in a Bayesian context (Friston et al., 2018).

It remains largely unknown how the brain mediates the balance between behavioural stability and flexibility. Previous work has investigated the role of dopamine signalling in regulating the balance between stability and flexibility, where dopamine the stimulation of D1 and D2 dopamine receptors in the prefrontal cortex is thought to promote behavioural stability and flexibility, respectively (Cools, 2019; Durstewitz and Seamans, 2008); recent work in humans has confirmed a causal role of dopamine in behavioural flexibility (Riedel et al., 2022). Interestingly, a considerable and growing body of work has also implicated neural variability (i.e. the variability of different measures of neural activity over time) in mediating corresponding behavioural variability (Armbruster-Genç et al., 2016; Fujino et al., 2017; Garrett et al., 2013, 2011; Nomi et al., 2017; Palva et al., 2013; Waschke et al., 2021, 2017). Indeed, in a recent review, Waschke et al. (2021) propose that neural variability is necessary for the brain to flexibly adopt different cognitive strategies for different situations – that is, neural variability is necessary for behavioural flexibility.

Given this relationship between neural variability and behavioural flexibility, it is reasonable to consider whether neural processes such as cortical oscillations and scale-free activity differ in their level of variability; this may predispose them to mediate flexible versus stable aspects of behaviour. In the present work, we take this approach to examine and compare scale-free and oscillatory activity with respect to their neural "stability" and "flexibility". We defined the "flexibility" of a neural process operationally, in terms of both its spontaneous fluctuations (neural variability as discussed above) and its propensity to change in in response to environmental demands. A "flexible" brain process is one that fluctuates spontaneously, and changes considerably in response to a variety of tasks. A "stable" process refers simply refers to the opposite end of this continuum, reflecting a process which changes little either spontaneously or in different cognitive conditions.

To compare oscillatory and fractal dynamics on the basis of stability and flexibility, we first quantified their responsiveness to external perturbations by examining changes in oscillatory and fractal parameters from resting-state to different cognitive task states, (referred to as rest-task change), and by measuring event-related changes in response to brief sensory stimuli. We focused on the parameters of oscillatory power, and the scaling exponent and broadband offset of scale-free activity. We quantified the coefficient of variation (CV) of different oscillatory and fractal parameters over time during resting-state; this provides a common metric that allows us to compare the spontaneous within-subject variability of fractal and oscillatory parameters independent of explicit cognitive demands. Finally, to assess whether features which exemplified neural stability were also consistent across subjects, or reflected individually-specific trait variables, we computed inter-subject variability as the between-subject CV of each parameter.

We hypothesized that cortical oscillations should show larger responses to external perturbations, greater spontaneous intra-subject variability, and greater inter-subject variability than scale-free activity. The multitude of findings examining changes in oscillatory power in tasks (Güntekin and Başar, 2016; Klimesch et al., 2006; Makeig, 1993) suggests that oscillatory activity likely reflects a flexible component of brain activity. In contrast, given its association with the self (Huang et al., 2016; Kolvoort et al., 2020; Wolff et al., 2018), the most stable and continuous aspect of our mental life (Northoff, 2017), and following recent fMRI findings showing consistent scale-free temporal hierarchies across and within subjects (Golesorkhi et al., 2021; Ito et al., 2020; Raut et al., 2020), we hypothesized that scale-free activity may reflect a stable component of neural activity. To investigate these hypotheses, we used MEG data from the Human Connectome Project (Larson-Prior et al., 2013) and the Cambridge Centre for Aging Neuroscience dataset (Shafto et al., 2014; Taylor et al., 2017).

In brief, we show that fractal parameters are generally more "stable" than oscillatory ones: that is, they show less responsiveness to tasks, less spontaneous intra-subject variability, and less inter-subject variability. In scale-free activity, this effect was generally driven by the high stability of the power-law exponent, while the power or amplitude of fractal fluctuations struck a balance between stability and flexibility. In the case of cortical oscillations, alpha power displayed the greatest flexibility, while other parameters were trait-like or displayed task-specific changes. Overall, our findings provide insights into how the brain balances the seemingly contradictory requirements of neural flexibility and stability using fractal and oscillatory electrophysiological dynamics. This difference can be interpreted in homeostatic terms, with scale-free activity serving the role of a homeostatically regulated variable, while cortical oscillations reflect "effectors" which serve to maintain regulated variables near their physiological set-point.

2. Methods

2.1. . HCP preprocessing and source reconstruction

Resting-state and task MEG data were obtained from the Human Connectome Project (Larson-Prior et al., 2013). The HCP MEG dataset contains data from 95 subjects in total, 89 of whom completed the three eyes-open resting state recordings (41 females, age $M = 28.6$, SD = 3.85). Of these, 77 completed the working memory task, 78 completed the story-math task, and 56 completed the motor task; these tasks each had two associated MEG recordings. Data were recorded on a MAGNES 3600 MEG system (4D Neuroimaging, San Diego, CA) with 248 magnetometer channels. For resting-state data, we took preprocessed data from the *rmegpreproc* stage of the HCP MEG preprocessing pipeline; briefly, this pipeline involves removing channels with low correlations with their neighbours and high variance ratio, and then removing artefactual components using an iterative ICA procedure. ICA components are classified automatically based on 6 parameters (including correlation with noise channels, flat spectra, and kurtosis; see Larson-Prior et al. 2013 for details) and non-brain components, reflecting eyeblink, muscle, or sensor artefacts, are removed. Bad segments were identified and removed based on their z-scored amplitude, flatness (no signal), and muscle artefacts, using built-in routines in Fieldtrip.

To analyze the task recordings (working memory, story-math, and motor) as a whole block, rather than analyzing stimulus- or event-

related changes, we then applied the HCP resting-state preprocessing pipeline to the task recordings using the megconnectome software (Larson-Prior et al., 2013). This ensured that differences between the recordings were not due to signal quality issues, and allowed us to analyze each task recording as a single continuous block. The working memory task consisted of ~30 s 0-back (match to sample) and 2-back blocks, interleaved with 15 s resting blocks (~1 min of task for each 15 s of rest; 2 10 min runs, 16 blocks per run). In the story-math task, participants are presented with sequences of sentences consisting of fables or math problems, and are then asked a comprehension-testing question at the end; resting blocks are negligible (22 story/math blocks per run, 2 7 min runs). During the motor task, participants are asked to tap their fingers or move their toes; movements occur in blocks of 12 s (32 motor blocks per 14 min run, 2 runs), with 9 15 s rest blocks per 7 min run.

To compute fractal and oscillatory power spectra at a source level, we computed source-level dipole moment time series using eLORETA (Pascual-Marqui et al., 2011), as implemented in the Fieldtrip toolbox (Oostenveld et al., 2011). We chose eLORETA because multiple studies have found that it performs favourably with respect to localization error relative to alternative strategies such as minimum-norm estimation or beamforming (Halder et al., 2019; Pascual-Marqui et al., 2018). For each subject, we used single-shell head models and 2-dimensional cortical sheet source models with 8004 vertices created in the HCP anatomy pipeline (Larson-Prior et al., 2013). In brief, single-shell head models were estimated from participants' individual MRIs using SPM8. Source models were created from cortical surfaces generated using Freesurfer's recon-all pipeline (Dale et al., 1999); these surfaces were nonlinearly warped to the normalized MNI template, and downsampled to a resolution of 4002 vertices per hemisphere (see Larson-Prior et al. 2013 for details). We then applied eLORETA to the full source-level time series; the spatial filter from this computation was applied to the data to compute source-level dipole moment time series at each vertex.

To reduce the dimensionality of our data, we next applied a cortical parcellation to reduce the vertex-level time series to region-level time series. We used the HCP multi-modal parcellation described in Glasser et al. (2016) for this purpose. The Glasser et al. parcellation is based on the convergence of multiple structural (myelin, cortical thickness), functional (responses to HCP tasks), and connectomic (resting-state functional connectivity) features, combined in a semi-automated pipeline and interpreted by trained neuroanatomists (Glasser et al., 2016). Region level time series for 360 regions were calculated by averaging the time series of all constituent vertices of the region. This procedure introduces rank deficiency into the data: however, as we were not concerned with connectivity, linear dependency between signals in different regions is not a major issue for our analysis. Nevertheless, we controlled for this by grouping the parcellation regions based on the grouping proposed in the supplement of Glasser et al. – this left 22 regions in each hemisphere, rendering the data full rank. The results of these analyses are reported in the supplementary materials.

2.2. Computation of fractal and oscillatory power spectra and power spectral features

Fractal and oscillatory power spectra were separated using the recently-developed Irregular Resampling for Auto-Spectral Analysis method (IRASA; Wen and Liu 2016b). IRASA decomposition was performed separately on each resting state and each task recording in the HCP dataset (3 resting states, 2 task recordings per task; see *HCP preprocessing and source reconstruction*, above). To ensure proper separation given non-stationary data, we applied the IRASA method in a 10 s sliding window with no overlap, following previous publications (Kolvoort et al., 2020; Muthukumaraswamy and Liley, 2018). The spectra from each 10 s window were averaged across windows to create the power spectrum for each condition. Again following previous work (Kolvoort et al., 2020; Muthukumaraswamy and Liley, 2018), we used a wider range of resampling factors to improve the separation of the oscillatory and fractal power spectra; these ranged from 1.1 to 2.9 in steps of 0.05, excluding 2. Because of the effect of filtering artefacts on the data, we analyzed a frequency range from 2 to 85 Hz.

We then decomposed these power spectra into a smaller number of features. We parametrized fractal power spectra as being composed of a slope (power-law exponent, or PLE) and a y-intercept. In contrast, oscillatory power spectra were divided into five conventional frequency bands (Buzsáki, 2006): delta (2–4 Hz), theta (4–8 Hz), alpha (8–13 Hz), beta (13–30 Hz), and gamma (30–85 Hz) (we also considered a version of the analysis where the alpha band was defined individually for each subject; these results are reported in Supplementary Figs. S17 and S18). To calculate the fractal parameters, we first linearly interpolated frequency values to be evenly spaced on a log-scale, to ensure that fitting a straight line would not be overly biased by a large number of high-frequency estimates (Wen and Liu, 2016b). The power-law exponent was then calculated as the slope of a linear fit of log-transformed power versus log-transformed (interpolated) frequency; the fractal amplitude was calculated as the y-intercept of this same linear fit (Wen and Liu, 2016b). Oscillatory power for each band was calculated as the area under the curve of the oscillatory power spectrum within each frequency range.

2.3. Statistical analysis of rest-task change indices

To assess changes in each oscillatory and fractal parameter from resting state to each of the three tasks, we compared resting-state and task values of each parameter (power in 5 oscillatory bands, slope and intercept of fractal activity) with Wilcoxon signed rank tests at each of the 360 regions of the Glasser et al. parcellation. Multiple comparisons across regions of the Glasser template were corrected for using false discovery rate (FDR) correction (Benjamini and Yekutieli, 2001). To assess the degree to which each fractal and oscillatory parameter was engaged in the task on a common basis, we then computed the percent change of each parameter from resting-state to task. We then took the median of these values across subjects, and summed the absolute values of these percent change values over all regions whose changes were significant after the FDR correction across regions described above; we will refer to this value as AbsPrcChange. This AbsPrcChange value was taken to reflect the degree to which a fractal or oscillatory parameter was modulated by the task, taking into account both the magnitude of the change as well as its spatial extent. To compare these values between parameters, we used a bootstrapping procedure. We first computed confidence intervals for each AbsPrcChange value using 10,000 bootstrap samples (resampling subjects), using the bias-corrected and accelerated bootstrap. We then created 10,000 bootstrap samples for the difference in the AbsPrcChange values between each pair of parameters, and computed a p-value for this difference using the bootstrap distribution, applying bias-correction and acceleration using the iboot package (Penn, 2020). The matrix of comparisons between parameters was then corrected for multiple comparisons using Bonferroni-Holm correction (Holm, 1979).

As discussed in the results section, we also considered a more strict criterion for rest-task change by considering the impact of differences between measures in spontaneous intra-subject variability. In a supplementary analysis, we took the deliberately unrealistic assumption that all intra-subject fluctuations are "noise" (or at least not variability of interest), and normalized the rest-task changes by the intra-subject SD rather than the resting-state mean value. We refer to these values as "Pseudo effect size" values, as they are similar to classical measures of effect size, which divide the mean effect by the inter-subject SD. The analysis then followed the same steps as above, using bootstrapping to create confidence intervals and compare the statistics between measures. We repeated this analysis a third time, this time using Cohen's *d* instead of the pseudo effect size measure. All of these results are reported in the supplementary materials.

We investigated in further detail the differences between the two fractal parameters. We defined "unique activations" for each parameter

as regions which showed a significant rest-task change for one parameter, but not the other. Further, we compared the rest-task percent change of fractal amplitude and PLE at each region using a Wilcoxon signed rank test, correcting for multiple comparisons with FDR correction. Finally, as a complement to the bootstrap analyses described above, we compared the median region's absolute percent change from rest to task between the fractal intercept and PLE using a Wilcoxon signed-rank test.

2.4. Time-resolved event-related fractal and oscillatory spectral changes

Using the CamCAN dataset (Shafto et al., 2014; Taylor et al., 2017), we next investigated stimulus-evoked changes in oscillatory and fractal parameters in a time resolved way. Preliminary results of this have been reported in a previous publication (Wainio-Theberge et al., 2020), and the methods are described in full there. A randomly selected subset of 195 subjects (105 females, age $M = 56.3$, SD = 15.3). from the original CamCAN dataset was analyzed here, since the time-resolved IRASA procedure is extremely computationally intensive. The preprocessing of the CamCAN data for rest-task analysis followed roughly the same procedure as described in a previous publication (Wainio-Theberge et al., 2020). CamCAN data were recorded on a 306-channel VectorView MEG scanner (Elekta Neuromag, Helsinki). In the initial CamCAN data release, temporal Signal Space Separation (MaxFilter 2.2, Elekta Neuromag, Helsinki) was applied to clean the data and correct for head motion in 200-ms time windows. Starting from this MaxFiltered dataset, we first removed gradiometer channels, focusing only on magnetometers. Data were then downsampled to 500 Hz, including anti-aliasing filtering, and notch filtered at 50 Hz, 100 Hz, 150 Hz, and 200 Hz. Autoreject (Jas et al., 2017) was then applied to remove high-amplitude artefacts prior to ICA decomposition. We then used an in-house adaptation of the HCP's megconnectome software to perform 20 iterations of ICA decomposition and reject components automatically; the same criteria as described above for the HCP data were used to reject components. Following ICA decomposition, data were epoched from −2 to 1.5 s around stimulus onset, and a second round of Autoreject was run to identify artefacts, repair them via interpolation, and reject bad trials.

Data were projected into source space using generally the same procedure as for the HCP data. To create the head model and source model, we used the outputs of FreeSurfer's recon-all pipeline (Dale et al., 1999). The head model was estimated as a single shell model from the intensity normalized T1 image from recon-all. To create the source model, the Freesurfer cortical surface was downsampled to 8004 voxels and nonlinearly warped to HCP fs_LR space (Van Essen et al., 2012), following the methods of the Human Connectome Project as implemented in the Fieldtrip routine *ft_postfreesurferscript.sh*. We then aligned these head models and source models with the MEG sensors using the fiducial locations provided with the CamCAN data release. Data were then projected to the source level using the same eLORETA procedure described for the HCP data. We then used the parcellated the data using a reduced version of the Glasser et al. (2016) multi-modal parcellation, in order to save computational time; this reduced version follows Glasser et al.'s grouping of their 360 parcels into 44 regions, described in the supplementary materials of Glasser et al. (2016).

We next computed the IRASA spectral decomposition in a 1.5 s sliding window. Our baseline period took windows centered from −1.25 s pre-stimulus to −0.75 s post-stimulus in steps of 25 ms; our post-stimulus period considered windows centered from 0 to 0.75 s poststimulus, again in steps of 25 ms. In order to exclude any effects of the previous stimulus on the baseline, we considered only trials where the preceeding ITI was longer than 4 s; this left on average 42 trials per subject. Computation of fractal and oscillatory parameters followed the same procedure as described above. A 1.5 s window was used as this was the minimum window size in order to be able to include 3 cycles of our lowest frequency (2 Hz), as recommended in the EEGLAB package (Delorme and Makeig, 2004).

We conducted two statistical procedures to assess stimulus-evoked changes of the oscillatory and fractal power spectra. First, we computed a standard analysis of event-related spectral perturbation (Makeig, 1993), by averaging the IRASA power spectra over all channels, and assessing changes at each frequency for the oscillatory and fractal power spectra, as well as the original "mixed" power spectra (oscillatory plus fractal). We conducted a Wilcoxon signed-rank test at each brain region, frequency, and post-stimulus time point, comparing each frequency with the mean value in the baseline period (−1.25 to −0.75 s pre-stimulus). We then corrected for multiple comparisons using a cluster based permutation test; a two-sided test was used with a cluster alpha of 0.025 and a channel-level alpha of 0.05 (Maris and Oostenveld, 2007). Next, we assessed changes in our original oscillatory and fractal features (oscillatory power in 5 bands, fractal intercept and PLE): we tested these changes at each channel and each post-stimulus time point with a Wilcoxon signed-rank test against the mean value of the parameter in the baseline period. Multiple comparisons were again corrected for with a cluster-based permutation test, this time over channels and time rather than frequencies and time. Finally, to compare the degree of post-stimulus change in each parameter, we again computed AbsPrcChange values for each band and fractal parameter, summing the absolute values of the percent change of each parameter over all regions and time points found significant with the cluster-based permutation test described above. We then computed bootstrap confidence intervals and differences between these AbsPrcChange values as described above, with one modification. As significance in the time-locked analyses was computed with a cluster based permutation test, it would be too computationally intensive to recompute significance in each bootstrap sample: therefore, we used the original significance mask in every bootstrap sample. We found in the HCP data that this approach gives similar results to the approach in which the significance mask is recomputed within each bootstrap sample.

2.5. Estimation of intra- and inter-subject variability

To calculate inter- and intra-subject variability of each parameter (fractal and oscillatory), we employed the coefficient of variation (CV). The coefficient of variation is a standardized measure of variability which is unitless and does not depend on the scale of the data (Koopmans et al., 1964). It is traditionally defined as the standard deviation of the data divided by the mean:

$$cv = \frac{\sigma}{\mu}$$

For log-normal data, the following modified formula is a more accurate estimator (Koopmans et al., 1964):

$$\hat{cv} = \sqrt{e^{s_{ln}^2} - 1}$$

Where s_{ln} is the standard deviation of the natural logarithm of the original data. Since the distributions of all of our measures (oscillatory power in all bands, fractal scaling exponent and intercept) exhibited considerable skewness, we applied this formula to estimate the coefficient of variation.

To calculate inter-subject variability in resting-state, we averaged the fractal and oscillatory parameters across regions and across resting-states and computed the coefficient of variation of each parameter across subjects. To calculate intra-subject variability, we computed the IRASA features as described above on each 10 s non-overlapping segment over which the IRASA was originally computed; segments from the three different resting-states were concatenated. For each subject, we then computed the coefficient of variation of each parameter across resting-state segments, and averaged the result across subjects to produce the mean intra-subject CV for each parameter.

To statistically compare intra- and inter-subject CV values between parameters, we followed a similar bootstrapping procedure as for the AbsPrcChange values. We computed bootstrap confidence intervals with

10,000 bootstrap samples for both the inter-subject CV and mean intra-subject CV values. We then computed p-values for the differences of inter-subject CV and mean intra-subject CV between parameters by computing 10,000 bootstrap samples of the difference values. These p-values were then corrected for multiple comparisons using Bonferonni-Holm correction, as above.

All code for the above analyses (including preprocessing of the CamCAN data) is available online at http://www.github.com/SorenWT/oscifrac2021.

3. Results

While multiple processes in the brain display scale-free dynamics, including cortical avalanches (Palva et al., 2013), oscillatory amplitude (Linkenkaer-Hansen et al., 2001), and network dynamics (Racz et al., 2019), perhaps the most obvious example of scale-free activity is the broadband distribution of the electrophysiological power spectrum (He, 2014; He et al., 2010). The power spectrum of electrophysiological recordings generally follows a $1/f^{\beta}$ distribution, with power decreasing with linearly on a log-log scale with increasing frequency (Eke et al., 2002). While these scale-free dynamics are perhaps the most comparable with oscillatory activity, comparing cortical oscillations and scale-free activity of this sort is methodologically challenging, as standard Fourier or wavelet methods of estimating the power spectrum do not distinguish between scale-free and scale-dependent processes. Recently, robust methods based on resampling (Wen and Liu, 2016b) and curve fitting (Donoghue et al., 2020) have been developed to separate oscillations and fractal/scale-free activity; these have been used to considerable effect in establishing differential functional and physiological roles for the two processes (Ouyang et al., 2020; Wen and Liu, 2016a).

While curve-fitting methods have showed considerable promise in recent years (Donoghue et al., 2020), we found that they were unsuited for our purpose due mainly to the arbitrary parameter setting involved in their use (see Limitations and future directions for more details); we therefore decomposed the mixed power spectrum into oscillatory and fractal components using the Irregular-Resampling for Auto-Spectral Analysis (IRASA) method (Wen and Liu, 2016b; see Fig. 1a for a schematic). The IRASA method was applied in a 10 s sliding window with no overlap, following previous publications (Kolvoort et al., 2020; Muthukumaraswamy and Liley, 2018).

We then divided the oscillatory component with 5 frequency bands (2–4 Hz delta, 4–8 Hz theta, 8–13 Hz alpha, 13–30 Hz beta, and 30–85 Hz gamma) and computed the average power over all 10 s segments, and assessed the fractal component with the fractal power law exponent, or PLE (slope of a straight-line fit of log power vs. log frequency) and fractal amplitude (this latter parameter can be assessed either as the y-intercept of the aforementioned straight-line fit (Donoghue et al., 2020), or simply as the average power of the fractal component in the frequency range of interest; we took the former approach in this paper, while the latter is reported in the supplementary materials). In this way, we were able to investigate not only differences between fractal and oscillatory dynamics, but also differences between different fractal parameters (like amplitude and power law exponent) within the fractal fluctuations themselves, something which has rarely been explored in the literature.

We directly compared the two fractal parameters with the different oscillatory measures in their degrees of flexibility and stability using our three metrics, that is, rest-task change, intra-subject variability, and inter-subject variability (see Fig. 1b for a schematic). For that purpose, we first probed flexibility and stability in the three Human Connectome Project MEG tasks, which consisted of a working memory N-back task, a verbal comprehension task ("story-math" task), and a simple motor tapping task (see Methods and Larson-Prior et al. 2013 for details). In this way, we directly compared oscillatory and fractal parameters as well as comparing the two fractal parameters to each other. Next, we examined sub-second scale changes in each of these parameters in response to brief, multisensory stimuli in the CamCAN MEG dataset (Shafto et al., 2014; Taylor et al., 2017). The CamCAN task required participants to respond as fast as possible when they heard or saw a simultaneously presented 300 ms tone or 34 ms visual checkerboard. Finally, we complemented these analyses by examining inter- and intra-subject variability in resting-state using the HCP dataset, quantifying this with the coefficient of variation, which was subsequently compared between oscillatory and scale-free parameters.

3.1. Fractal PLE changes less during task states than oscillatory components

We first investigated whether fractal and oscillatory components differ with respect to their activation in different cognitive tasks in the Human Connectome Project MEG dataset. Fractal and oscillatory parameters differed in both the topography and magnitude of their task-evoked changes. The three different tasks (working memory, story-math, motor) showed different topographic patterns of rest-task change between oscillatory and fractal components, with oscillatory components generally showing more global changes (see Fig. 2). Most importantly, the magnitude of rest-task change differed between oscillatory and fractal dynamics: rest-task change was usually highest for oscillatory alpha, intermediate in fractal amplitude and the other oscillations, and lowest in PLE (see Fig. 2). Together, these results show that oscillatory and fractal components differ in their responsiveness to task, and that oscillatory components show greater rest-task change than fractal components of the power spectrum: this effect is particularly pronounced for the alpha band and the PLE.

We next focused specifically on the two fractal parameters, PLE and fractal amplitude, with respect to the topography and magnitude of their task-evoked modulations. These results demonstrate that the PLE and amplitude show differing topographies in their task-related activations (Fig. 3). Most notably, in every task, despite the task-specific directions of changes (i.e. increases vs. decreases in different tasks) and regions involved, the fractal amplitude consistently showed larger magnitudes of change than the PLE across a wide number of regions, including in regions which coactivated the two measures.

For both of the previous analyses, we conducted several control analyses for robustness. We repeated these analyses in (a) the CamCAN dataset, which employed a less cognitively-demanding task (Supplementary Fig. S11), (b) in the 44-region reduction of the MMP atlas (Supplementary Figs. S12 and S13), (c) using total fractal power instead of the fractal intercept (Supplementary Figs. S7 and S8), and (d) using measures of effect size instead of percent change (Supplementary Figs. S1–S3); these results broadly support the findings observed here.

3.2. Fractal PLE exhibits smaller sub-second stimulus-related changes than oscillatory dynamics, fractal amplitude

We next examined whether the changes we observed on long-time scales (block-level rest-task analysis) also held at the sub-second time scales relevant for processing short sensory stimuli. This is important, as the different frequency ranges involved in the different oscillatory and fractal parameters may predispose different time scales over which they may act. To this end, we used the multisensory stimulation task from the CamCAN dataset and examined fractal and oscillatory components in a sliding-window analysis, analyzing changes in these components in the 0 to 0.75 s post-stimulus period relative to a remote baseline from 1.25 to 0.75 s pre-stimulus (see Methods for details). We considered both a standard time-frequency analysis of changes in power, as well as our parametric analysis as above. With respect to power, the mixed power spectrum showed a stimulus related increase in slow-frequency power (2 Hz to 8.1 Hz at peak, frequencies vary by time and region; $p = 0.001$) and decrease in fast frequency power (6.8 Hz to 44.9 Hz at peak; $p = 0.001$), as commonly observed (Makeig, 1993); the slow-frequency power increase was generally centred over the left somatomotor cortex, while the fast-frequency power decrease was centered over

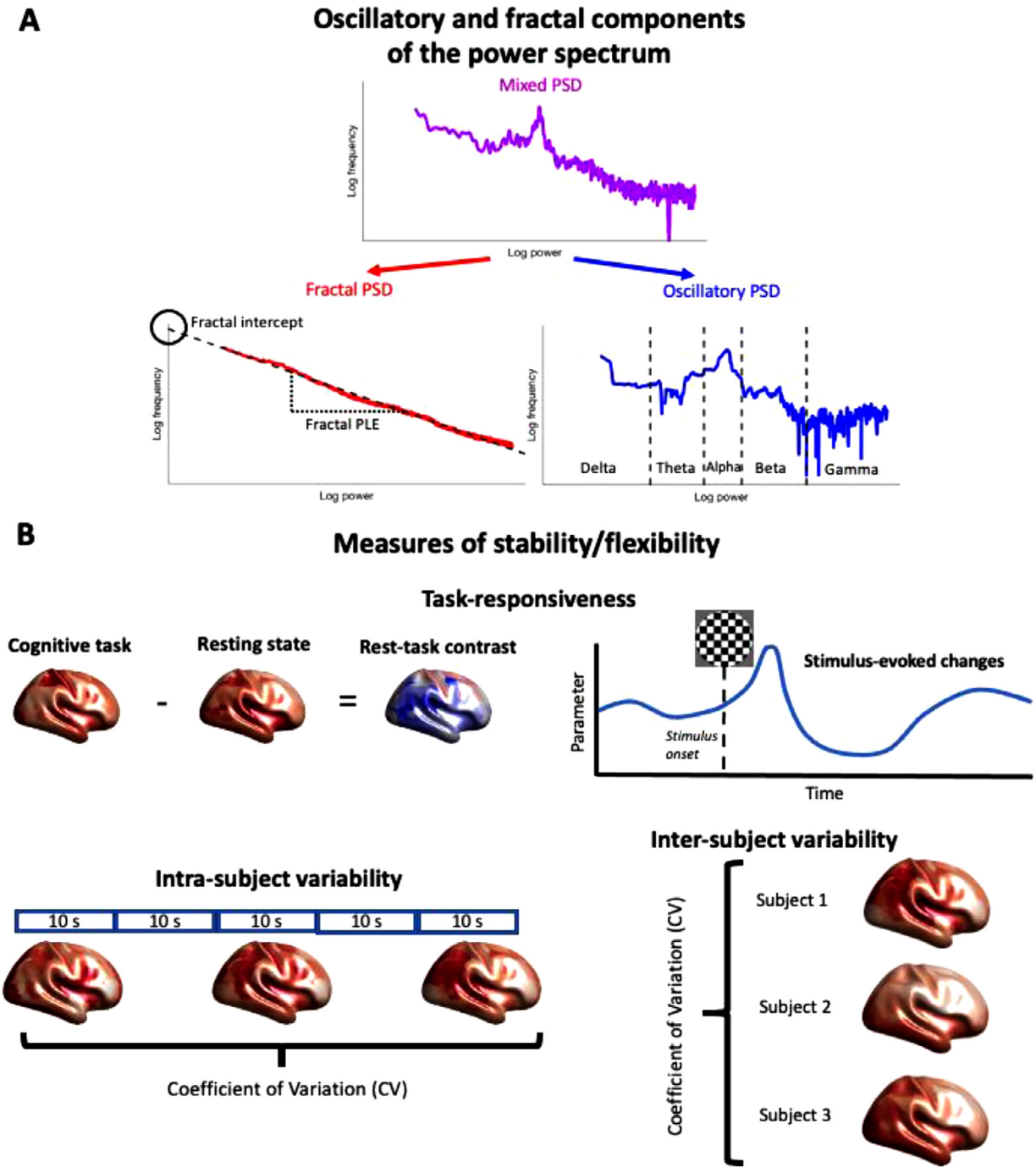

Fig. 1. Schematic of the study rationale and methodology. (A) Schematic of the power spectrum decomposition and calculation of parameters. Mixed power spectra were separated into oscillatory and fractal components using a resampling based procedure (see Methods). The oscillatory PSD was then parametrized in terms of the five conventional frequency bands (delta, theta, alpha, beta, gamma), while the fractal PSD was operationalized in terms of its slope (PLE) and fractal amplitude. (B) Schematic of the methods of the study. We systematically examined task-responsiveness (a facet of intra-subject variability), inter-subject variability, and intra-subject variability, and conducted a preliminary genetic analysis to examine sources of inter-subject variability, in fractal and oscillatory dynamics.

the bilateral posterior cingulate gyrus and visual cortex (Fig. 4a). Findings for oscillatory power were virtually identical, with a slow-frequency increase in power over somatomotor regions ($p = 0.001$; 2 Hz to 8.1 Hz at peak) and a fast-frequency decrease in power over posterior cingulate and visual regions (6.8 Hz to 44.7 Hz at peak; $p = 0.001$). Fractal power showed a similar pattern, but with differing frequency ranges and topographies. While the slow-frequency increase showed a similar topography as the oscillatory component, it extended over a larger frequency range (2 Hz to 16.6 Hz; $p = 0.001$); meanwhile, the fractal power fast-frequency decrease was centered over the motor cortex, and likewise showed an extended frequency range (15.9 Hz to 85 Hz at peak; $p = 0.001$).

We next took the parametric view described above and computed changes with respect to the time courses of fractal parameters (amplitude, PLE) and oscillatory parameters (delta, theta, alpha, beta, gamma power) (Fig. 4b). We observed that fractal amplitude and PLE both increased post-stimulus ($p = 0.001$, cluster-based permutation test); fractal amplitude increased markedly by 75%, while PLE increased only by 9%.

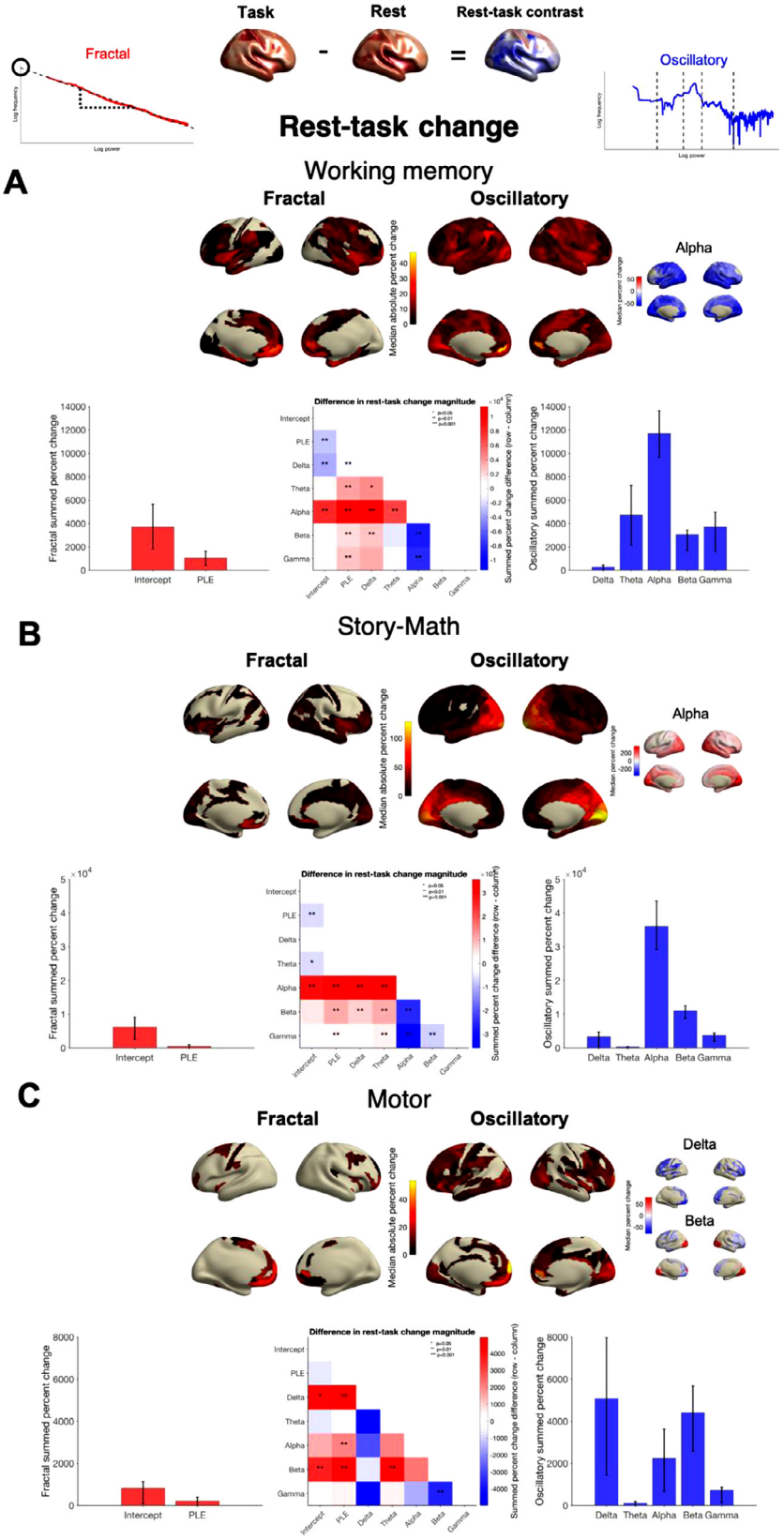

Fig. 2. Fractal and oscillatory changes from rest to task in the HCP (A) working memory, (B) story-math, and C) motor tasks. Absolute percent change values from rest to task were calculated as described in the text: surface plots show the topographical distribution of these values, averaged over fractal (left) and oscillatory (right) parameters, masked for significance within each parameter. Insets on the right show the median percent change of the most relevant oscillatory parameters (those for fractal parameters are shown in greater detail in Fig. 3). Accompanying bar plots show the summed absolute percent change values over all regions for each parameter: error bars indicate bootstrap 95% confidence intervals. The difference matrix below presents the differences of these summed absolute percent change values between parameters: each cell reflects the parameter in the row minus the parameter in the column. Significance of each difference is indicated with an asterisk: $^{*} = p < 0.05$, $^{**} = p < 0.01$. All p-values are Bonferroni-Holm corrected.

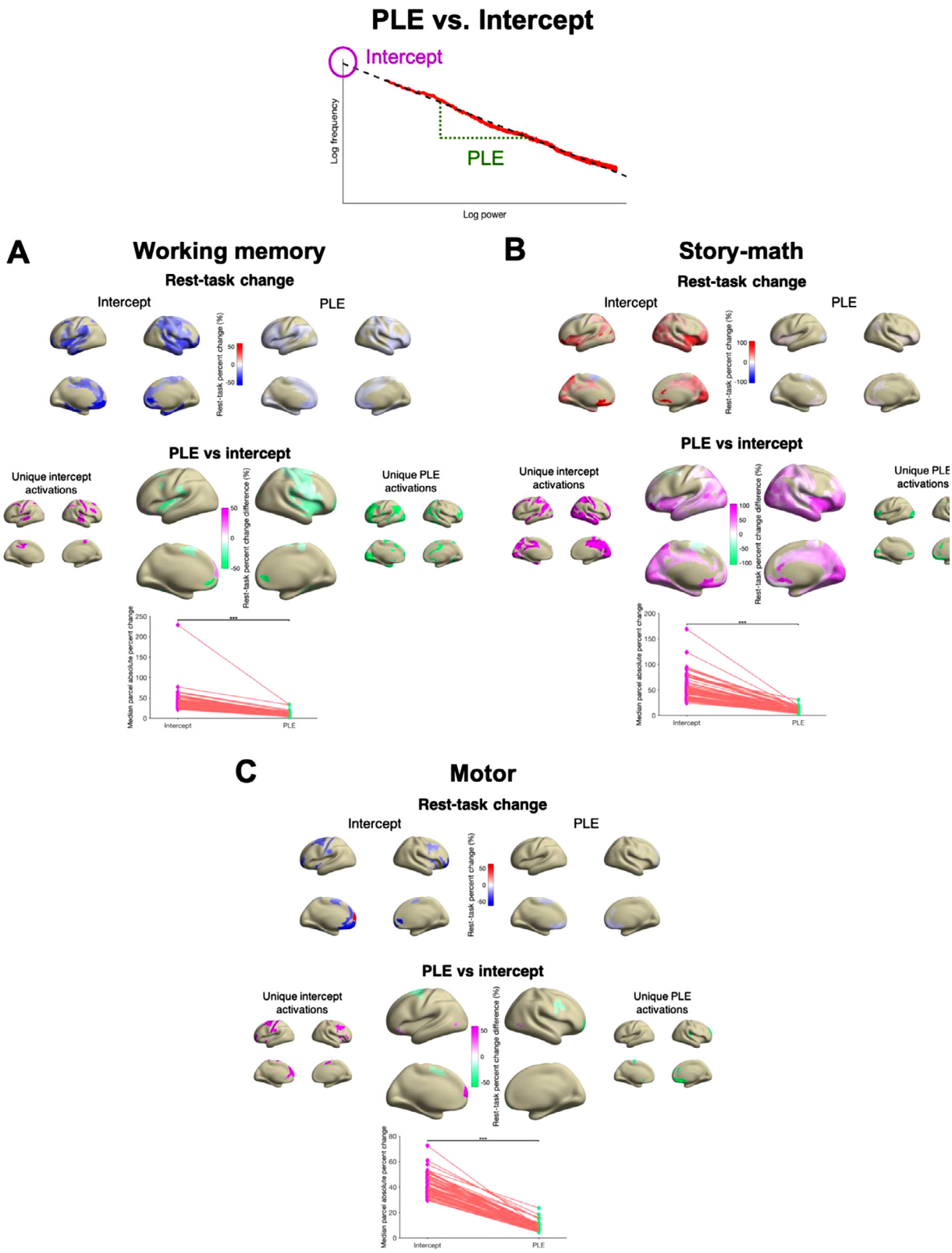

Fig. 3. Rest-task changes and differences between the two fractal parameters, fractal amplitude and fractal power-law exponent (PLE), for (A) working memory, (B) story-math, and (C) motor tasks (HCP dataset). Top set of surface plots show the actual rest-task percent change values, masked for significance (FDR corrected at $q < 0.05$), for fractal amplitude (left) and fractal PLE (right). Below, differences in the above percent change values (amplitude minus PLE) are plotted in the middle: pink indicates larger (more positive) values for amplitude, while green indicates larger (more positive) values for PLE. Plots are masked for significance of the difference in percent change values, FDR corrected at $q < 0.05$. On either side, unique activations for the amplitude (left) and PLE (right) are plotted, defined as regions where one variable is shows significant rest-task modulation while the other does not. Below, the median absolute percent change across parcels of the intercept (pink, left) and PLE (green, right) is indicated: each diamond represents a subject, and lines connect the same subject. Red lines indicate that the value is higher for the intercept than for the PLE, while blue lines indicate that the value is higher for the PLE than the intercept. Asterisks indicate significance according to a Wilcoxon signed-rank test: $^{*} = p < 0.05$, $^{**} = p < 0.01$, $^{***} = p < 0.001$.

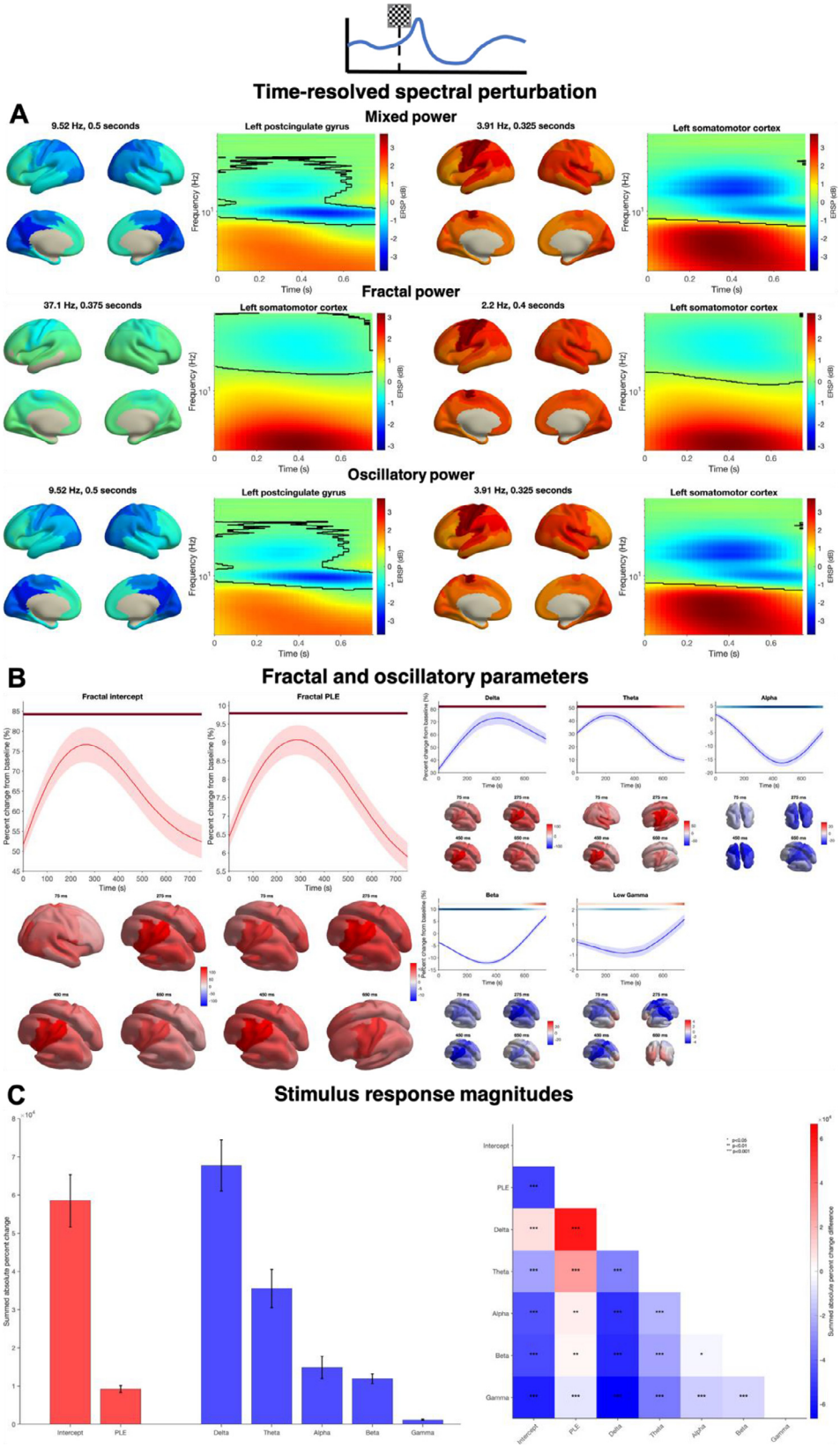

Fig. 4. Time resolved changes of oscillatory and fractal components. (A) Time-frequency plots and source topographies of mixed, fractal, and oscillatory changes following stimulus onset. Colours indicate change from baseline (−1250 to −750 ms), expressed in decibels; y-axis is log-scaled in order to better visualize the low-frequency response. Topographies are plotted at the peak time-frequency point of the cluster (i.e. the maximum absolute change); time-frequency plots are likewise plotted at the region where this peak is found. Outlined areas in the time-frequency plots form part of a significant cluster identified using a cluster-based permutation test. All clusters were significant at p= 0.001. (B) Parameter time courses for fractal (left) and oscillatory (right) components. Lines show time course of percent change of that parameter, averaged over subjects: shaded area indicates standard error. Topographies show the topography of the effect at four latencies throughout the poststimulus period (75, 275, 450, and 650 ms). Significance is indicated using graded overbars (red for positive clusters, blue for negative clusters); the colour of the bar reflects the percentage of regions which form part of a significant cluster at each time point (solid = all regions significant, white = no regions significant). (C) Summed absolute percent change statistics for each parameter, obtained by summing the percent change values over all time points and sensors in a significant cluster. Error bars indicate bootstrap 95% confidence intervals. Difference matrix (right) indicates the difference between the summed absolute percent change statistics, expressed as the parameter in the row minus the parameter in the column. Asterisks indicate significance of the difference: * = p < 0.05, ** = p < 0.01, *** = p < 0.001.

The oscillatory parameters showed relatively larger changes than the PLE, with delta increasing post-stimulus by a maximum of 72%, theta increasing by a maximum of 45%, and alpha and beta decreasing by 18% and 13%, respectively. Beta also showed both an late post-stimulus increase of 6% ($p = 0.0490$), while gamma showed an initial decrease of 1% and a subsequent increase of 1% ($p = 0.001$ for all changes except where otherwise marked, cluster-based permutation test with 2000 permutations).

Finally, we computed measures of the magnitude of stimulus-evoked change for each parameter in the same way as previously (Fig. 4c). PLE showed the second lowest absolute percent change value, lower than any measure but gamma, while delta power showed the largest change ($p < 0.01$ in each case); the fractal amplitude showed an average degree of change. Similar to the rest-task change results, this suggests that relative to most cortical oscillations (with the exception of the gamma band, which appears relatively stable), the fractal PLE is a stable parameter which responds minimally to tasks. As with the other analyses, we repeated these analyses using Cohen's *d* - these results are presented in the supplementary materials (Supplementary Fig. S4).

3.3. Fractal PLE shows lower intra- and inter- subject variability than oscillations and fractal amplitude

We next compared fractal and oscillatory dynamics based on inter- and intra-subject variability in resting state. We found that, in general, fractal parameters, particularly the PLE, displayed lower intra-subject variability than oscillatory ones, with the exception of the fractal amplitude having higher intra-subject variability than beta or gamma band power (Fig. 5a). The power-law exponent displayed by far the lowest intra-subject variability, significantly lower than all other measures ($p < 0.01$ in each case, Bonferroni-Holm corrected). In contrast, the highest intra-subject variability was found in alpha band power, significantly higher than all other bands ($p < 0.05$ for theta, $p < 0.01$ for all other bands).

Broadly similar results were obtained for inter-subject variability (Fig. 5b). Alpha power again displayed the highest inter-subject variability (higher than all others except theta, $p < 0.05$ vs. delta, $p < 0.01$ vs. all others), and PLE again displayed the lowest ($p < 0.01$ vs. all others). The fractal amplitude again displayed low-to-average inter-subject variability, higher than PLE and gamma power, but lower than delta, theta, and alpha power ($p < 0.01$ for each).

We conducted similar control analyses for robustness as in the task-related findings; these results are found in the supplementary materials. We computed a "normalized" inter-subject variability by dividing inter-subject variability by intra-subject variability, treating the latter as an estimate of noise rather than physiologically meaningful information (Supplementary Fig. S5); we also performed the same analyses in the CamCAN resting state recordings as well (Supplementary Fig. S11). Despite the overcompensatory normalization procedure, and the CamCAN resting state being eyes closed vs. the HCP's eyes open, the findings above remained broadly the same.

3.4. . Relative values of intra- and inter-subject variability: PLE as background, alpha as foreground

To summarize these results, we plotted inter-subject variability, intra-subject variability, and task-responsiveness of each measure (averaged across HCP tasks; Fig. 6a). The results clearly show that PLE shows the lowest inter- and intra-subject variability and the lowest task-responsiveness, while alpha power shows the highest values of all three parameters. We projected these results into two dimensions by aggregating our two intra-subject measures: the "aggregate intra-subject variability" metric in Fig. 6b represents an average of the z-scored values of task-responsiveness and intra-subject variability from Fig. 6a. Again, we see that PLE displays the lowest inter- and intra-subject variability, while alpha displays the highest. Interestingly, we also noted that the patterns of variability exhibited by most of the measures did not accord with traditional state-trait models of variability (Steyer et al., 2015), where measures are conceived to vary primarily in one or the other of intra- and inter-subject variability, but not both. Instead, measures tended to cluster along the diagonal of the intra- inter-subject variability matrix. In the discussion below, we term measures "background" and "foreground" measures: "background" measures have low intra- and low inter-subject variability, while "foreground" measures have high intra- and high inter-subject variability. We also repeated this visualization in our control analyses which treated spontaneous intra-subject fluctuations as noise: these results are reported in the supplementary materials (Supplementary Fig. S6), and generally agree with the present findings.

3.5. Genetic analysis of PLE and fractal amplitude

To further investigate the distinction between the fractal PLE and amplitude, we compared their genetic heritability. Recruiting the monozygotic vs. dizygous twin information from the HCP dataset ($n = 19$ and $n = 13$, respectively), we therefore calculated heritability indices for PLE and fractal amplitude, which quantify the extent of additive genetic contributions to each variable – these results are reported in the supplementary materials (Supplementary Fig. S15). In brief, PLE displayed moderate heritability (0.497; CI 0.160–1), while the fractal amplitude displayed low heritability which was not significantly different from 0 (0.296; CI −0.0298–1). This reinforces our finding of differences between the two fractal parameters (PLE and amplitude) with respect to their flexibility – however, we urge caution in the interpretation of these results, as our sample size for these analyses was very small ($n = 19$ monozygous twins and $n = 13$ dizygous twins).

4. Discussion

Scale-free and oscillatory activity are two central phenomena which can be observed in electrophysiological recordings, but their roles are rarely directly compared. Based on previous literature, we hypothesize that scale-free activity and cortical oscillations exhibit different trade-offs between stability and flexibility. We defined stability and flexibility operationally, in terms of a parameter's variability over time and over participants, and in terms of its responsiveness to external perturbations such as experimental stimuli. We tested our hypothesis by comparing scale-free activity and oscillatory power on the basis of their variability and task-responsiveness in two large-scale MEG datasets (the HCP dataset and the CamCAN study). Our study suggests that parameters of scale free activity and oscillatory power display different profiles of variability, which suggests distinct roles with respect to stability and flexibility in the brain.

We show that oscillatory power in general, and the alpha band in particular, is adaptive and flexible, exhibiting large task-related changes as well as high degrees of both intra- and inter-subject variability. In contrast, scale-free activity, especially the power-law exponent, is more stable, showing small task-related changes and low degrees of both intra- and inter-subject variability. Together, these data suggest that scale-free activity provides a more stable, facilitating neural background for the more flexible and adaptive oscillatory activity at the surface. Accordingly, these two components of electrophysiological activity may thus be related to stable or flexible aspects of behaviour.

4.1. Fractal scaling exponent is stable, alpha oscillations are flexible

Our results indicate that changes in the power of cortical oscillations, particularly in the alpha band, are well-suited to facilitate the brain's flexible responses to environmental stimuli. In our results, alpha band power consistently showed greater task-related changes than the majority of other oscillations or scale free parameters; it also showed greater inter- and intra-subject variability. This is in line with a large body of evidence relating alpha band modulations to performance in numerous

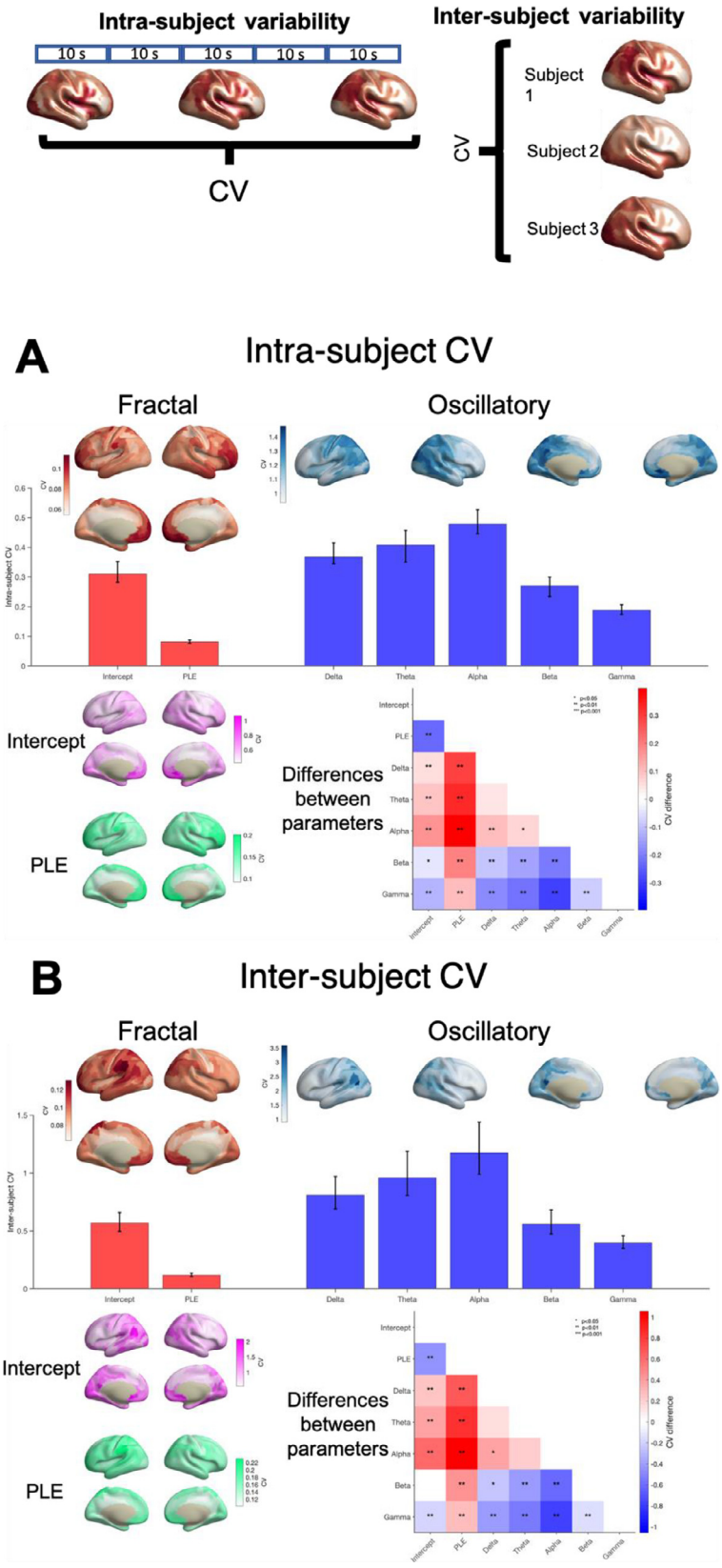

Fig. 5. Resting-state inter- and intra-subject variability of fractal and oscillatory parameters in the HCP dataset. Panel (A) shows intra-subject variability, panel (B) shows inter-subject variability. In each panel, bar plots show the whole-brain average coefficient of variation for each parameter (fractal parameters in red, oscillatory in blue). Above, the topographical distribution of the CV is plotted, averaged over parameters for fractal (left, red) and oscillatory (right, blue). Below the fractal parameters, the CV topography is plotted for the fractal amplitude (top, pink) and fractal PLE (bottom, green) separately. Right, the difference in coefficients of variation is plotted: as in Fig. 2, each cell reflects the CV of the parameter in the row minus the CV of the parameter in the column. Asterisks indicate significance of the difference: $^{*} = p < 0.05$, $^{**} = p < 0.01$, $^{***} = p < 0.001$. All p-values are Bonferroni-Holm corrected.

tasks (Fodor et al., 2020; Knyazev, 2007; Maguire et al., 2010; Palva and Palva, 2007), as well as to broad factors involved in responsiveness to stimuli such as attention (Klimesch, 2012, 1999). Further, individual differences in alpha power are also well-investigated, having been related to variation in attention (MacLean et al., 2012; Pitchford and Arnell, 2019), internally-guided decision making (Wolff et al., 2019), insight-oriented problem solving (Kounios et al., 2008), as well as trait variables such as anxiety (Knyazev et al., 2004). The present account of alpha as a mediator of neural flexibility also accords well with previous empirical and modelling work considering alpha as an important vari-

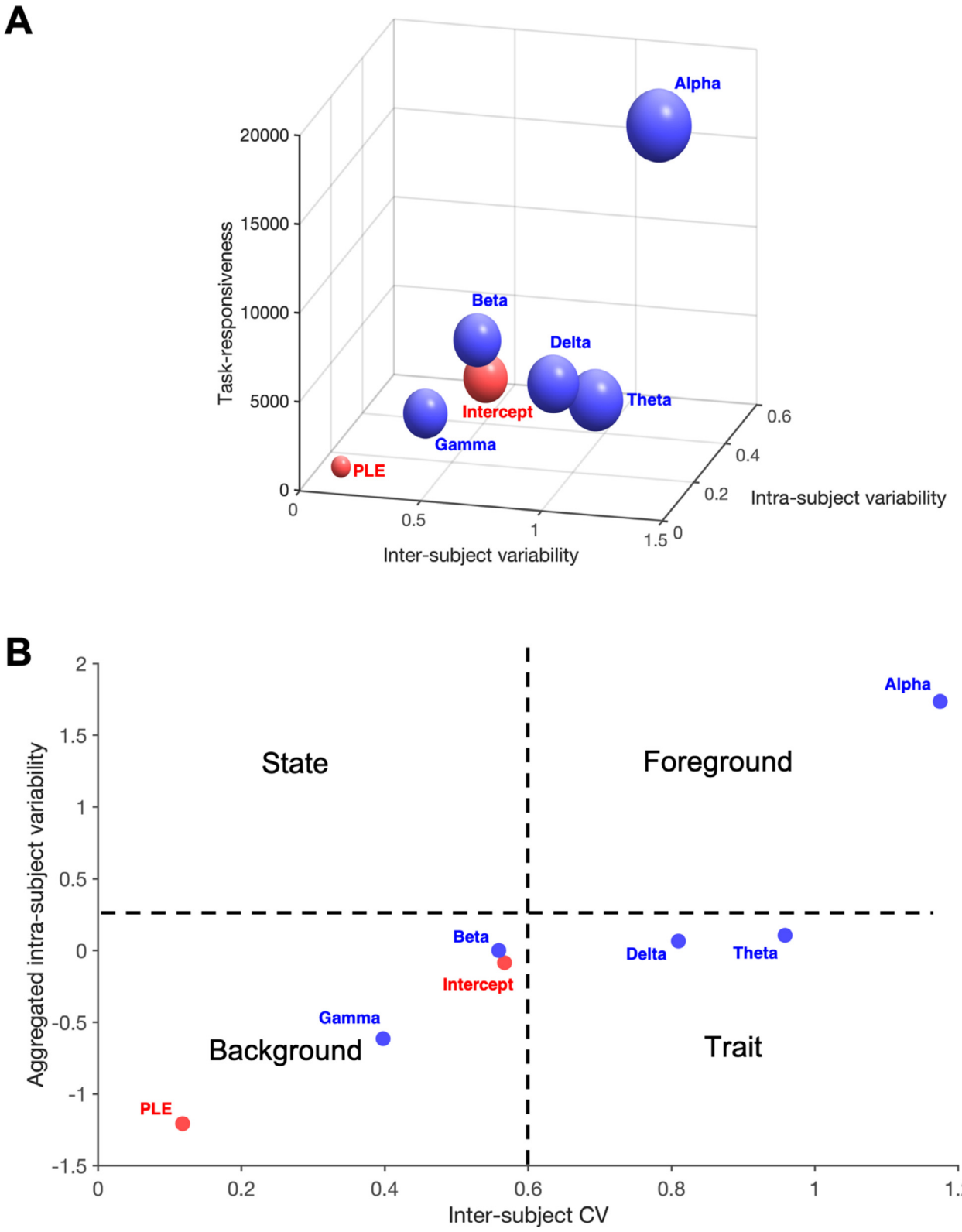

Fig. 6. Variability space for the fractal and oscillatory parameters assessed in the study. (A) 3D variability plot with inter-subject variability (CV, Fig. 5), intra-subject variability (CV, Fig. 5), and task-responsiveness (summed absolute percent change, Figs. 2 and 3) plotted as axes. Each parameter is plotted as a sphere, with fractal parameters in red and oscillatory in blue; size of the sphere is proportional to the distance to the origin, and thus reflects the total variability and task-responsiveness of the parameter. (B) 2D variability plot of intra- and inter-subject variability. Aggregated intra-subject variability reflects the average of the z-scored values of task-responsiveness and intra-subject CV in panel A. Each parameter is plotted as a point based on the values obtained in the text. Qualitative distinctions between different types of variables are overlaid. "Background" and "foreground" measures are a novel terminology introduced in the main text for measures which do not conform to standard "state" and "trait" variability; "background" measures have low intra- and low inter-subject variability and may play facilitatory roles in neural activity, while "foreground" measures have high intra- and inter-subject variability and may play a more active functional role.

able in processing sensory inputs (Cohen, 2014; Foxe and Snyder, 2011; Kim and Lee, 2019). Our findings extend this work by quantitatively comparing alpha power's stability and flexibility to other electrophysiological parameters, demonstrating the alpha band's potential role in mediating behavioural flexibility.

Alpha's dominant role in mediating flexible responses to tasks stands in contrast with the task-specific findings in other bands. While beta and delta oscillations were engaged mainly in the motor task (as well as delta in the CamCAN task), alpha was modulated consistently by all tasks (though to a lesser degree in the motor task). The task-unspecific nature of alpha power modulations is likely a large part of why alpha power appears highly flexible. In Klimesch (2012)'s model, alpha band activity reflects selective access to the "knowledge system", a general term encompassing both long-term memory and other forms of procedural and implicit knowledge; alpha band activity thus underlies many other cognitive processes, and reflects a general aspect of stimulus response. In contrast, other frequencies such as theta and beta oscillations have typically seen more circumscribed roles, such as beta's involvement in motor coordination (Jenkinson and Brown, 2011) or theta's involvement in memory tasks (Herweg et al., 2020). Our findings thus provide further support to the notion that modulations of alpha band power are a central way in which the brain responds flexibly to a variety of external stimuli.

In contrast to the flexibility of oscillatory power, our results demonstrate that scale-free activity is uniquely stable among electrophysiological parameters. The power-law exponent in particular, while exhibiting some limited task-related changes, generally shows the smallest magnitudes of response to a variety of tasks and experimental conditions; it also demonstrates low intra- and inter-subject variability. This result is in line with theories of scale-free activity which follow the framework of self-organized criticality (Beggs, 2008; Chialvo, 2010; Cocchi et al., 2017; Hesse and Gross, 2014). Criticality-based theories of scale-free activity posit that the brain is poised on the brink of a supercritical phase transition, a point at which the system's dynamics switch from damped fluctuations to sustained oscillatory behaviour (Cocchi et al., 2017). The notion that scale-free activity can only exist within a limited range (i.e. close to the critical point at which the phase transition occurs) is thus consistent with our finding of high stability in the power-law exponent, and suggests that maintenance of the brain near this critical point is relevant for neural functioning.

Given that scale-free activity is observed in numerous other systems, as discussed above, it may be that the stability of scale-free activity is not relevant for the brain; that is, while scale-free activity may be stable due to the same influences that produce scale-free activity in other systems, this may not mean that it has anything to do with promoting or effecting stable aspects of behaviour. However, our present results joins with considerable previous work to suggest that scale-free activity may indeed be relevant for behavioural stability. Scale-free activity has been shown to be predictive of self-consciousness (Huang et al., 2016; Wolff et al., 2018), as well in the processing of self-related stimuli (Kolvoort et al., 2020); this suggests that scale-free activity is involved in a highly stable aspect of mental life. Moreover, scale-free activity is known to be altered in schizophrenia (Ferri et al., 2017; Northoff et al., 2020), where dopamine signalling, a previously-discussed influence on behavioural flexibility (Riedel et al., 2022), is also abnormal (McCutcheon et al., 2020). Combined, these findings suggest that scale-free activity may be relevant for behavioural stability; however, future work is needed to make this relationship explicit and rule out the influence of external factors.

4.2. . Fractal dynamics – power vs structure

Our results also indicate a dissociation in function between different aspects of scale-free activity. Owing to the methodological difficulty of assessing broadband fractal power in distinction from oscillations, most work on scale-free activity in recent years has focused on the power-law exponent, or scaling exponent, of scale-free activity. The present paper is one of the first to additionally examine the fractal amplitude, a measure of the amplitude of broadband scale-free fluctuations. We show that the power of these broadband fluctuations exhibits considerably greater flexibility than the power-law exponent, a measure of their regularity. This indicates that it is the structure of the power spectrum, i.e., the scale-free relationship of power across different frequencies, rather than power itself that exhibits neural stability.

In this work, we also show a high-resolution, time-resolved decomposition of oscillatory and fractal activity in response to stimuli; these results were previously reported in part in (Wainio-Theberge et al., 2020). Using this analysis, we demonstrate that the power-law exponent and fractal amplitude both increase following stimulus onset. Given the power-law exponent's relation to excitation-inhibition balance (Lombardi et al., 2017, 2012; Poil et al., 2012), we suggest that this may reflect slight alterations in global excitation or inhibition induced by stimulus processing. However, in keeping with our main hypothesis, this effect was small, with PLE being modulated only by about 9%; this suggests, like our analyses in rest and task in the HCP dataset, that the PLE is buffered from external perturbations to a stronger degree than fractal power (75%) and oscillatory power (ex. alpha, 18%).

4.3. . Stability and flexibility in the brain: state vs. trait or background vs. foreground?

The present discussion of distinct neural components subserving neural stability and flexibility raises the common distinction with respect to psychological and behavioural outputs of states and traits (Steyer et al., 2015): state measures are intra-subjectively variable, but inter-subjectively consistent with respect to the driving external stimulus, while trait measures are intra-subjectively stable and inter-subjectively variable (Chaplin et al., 1988). Intuitively, it may seem that "stable" measures reflect trait variables, while "flexible" measures reflect state variables. However, this does not appear to be entirely consistent with our data.

If we consider inter-subject variability and intra-subject variability to be the x and y axes of a grid, then state variables lie in the upper left quadrant, and trait variables lie in the bottom right (see Fig. 6b). This leaves open the other two quadrants of the grid, the ones along the diagonal: we suggest that these quadrants may be termed "background" (bottom left) and "foreground" (top right). "Background" measures are thus those that display low within-subject variability *and* low between subject-variability, while "foreground" measures are those that display high within-subject variability *and* high between-subject variability; this is in contrast to state and trait variables, for which within-subject and between-subject variability are anticorrelated or mutually exclusive. Interestingly, in our data, most measures tended to fall along the diagonal of this plot, with few exhibiting the conventional patterns of "state" or "trait" variability. This suggests that the partitioning of stability and flexibility in neural dynamics does not necessarily follow intuitive notions of state and trait variability as defined in the psychological literature.

How can we distinguish neural background vs foreground measures, if they do not accord with state or trait models of variability? Background measures tend to show comparatively little variability both between and within subjects, i.e., low intra- and inter-subject variability. Functionally, background parameters change little in response to external perturbations: they thus may play facilitating or predisposing roles in cognitive and behavioural processes, but perhaps not direct and causal (i.e., sufficient) ones. This is similar to recent concepts of "neural predisposition" defined for consciousness (Northoff, 2013; Northoff and Heiss, 2015; Northoff and Lamme, 2020), and is consistent with previous investigations of scale-free activity, which have demonstrated that it can predict subsequent task-related activity (Huang et al., 2017; Kasagi et al., 2017; Scalabrini et al., 2019).

Foreground parameters, in contrast, are both inter-subjectively variable and more adaptive, i.e., responsive to environmental conditions: being more flexible, they may be directly involved in perception and cognition, providing their neural correlates as well as simultaneously mediating their inter-individual differences. This account is consistent with the litany of functions and associations ascribed to the alpha band, the canonical example of a foreground parameter in our data.

It is also possible, however, that the background and foreground categorizations mentioned here reflect mainly the influence of unsystematic noise. Indeed, when considering our control analyses where spontaneous intra-subject fluctuations were treated as noise, a number of oscillations fell into the "trait" category, rather than background or foreground (Supplementary Fig. S6). However, both scale-free measures remained as "background" parameters, and alpha power remained as a "foreground" parameter. As further advances in signal processing allow for the removal of more unsystematic noise from neural recordings, future analyses may show that more background and foreground parameters emerge as mainly state or trait; indeed, this would be consistent with studies such as Ouyang et al. (2020) which show meaningful behavioural consequences of individual differences in scale-free activity. However, for the moment, the possibility of a different models of variability from the psychological state-trait dichotomy cannot be ruled out.

4.4. . Power-law exponent vs. alpha oscillations: regulated variable vs. effector?

It must be mentioned that the properties of "background" and "foreground" processes we describe here overlap considerably with physiological distinctions between regulated variables and effectors (Modell et al., 2015). Regulated variables are those which are maintained within a narrow, optimal range by homeostatic mechanisms; in contrast, effectors are more readily modulated, changing to serve the goal of maintaining the regulated variables within their optimal range. Consider, for example, core body temperature (a regulated variable) and skin temperature (an effector). Core body temperature must be maintained within an extremely narrow range in order for metabolic processes to proceed optimally; in contrast, skin temperature readily adapts to environmental conditions such as the temperature outside, and displays high variability.

In keeping with our study, recent work has argued on computational and empirical grounds for distinguishing regulated variables and effectors on the basis of their patterns of variability (Fossion et al., 2018a, 2018b): effectors should display high variability and large responses to external perturbations, while regulated variables should display relatively low variability and little response to external inputs. Our results thus support the view that fractal dynamics, in particular the power-law exponent, function like regulated variables which are maintained near a specific set-point; in contrast, cortical oscillations like alpha function more like effectors, given their large variability. Future work should investigate the physiological underpinnings of this distinction: for example, if the power-law exponent reflects a regulated variable, one could investigate what mechanisms or sensors exist for keeping it within its optimal range.

4.5. . Limitations and future directions

In contrasting scale-free and oscillatory dynamics, we focused on one particular signal which displays scale-free behaviour, namely the "raw" field strength signal in MEG. This signal is known to reflect synchronous post-synaptic potentials, particularly from tangentially oriented sources (Ahlfors et al., 2010; Luck, 2014). However, many other processes are known to display scale-free fluctuations, including cortical avalanches (Palva et al., 2013), haemodynamic signals (He, 2014), dynamic functional connectivity (Racz et al., 2019), and, most notably, even the amplitude envelopes of cortical oscillations themselves (Linkenkaer-Hansen et al., 2001). As such, it may not be possible to generalize from our findings to the stability of other forms of scale-free activity in the brain. Future work should investigate the relationships between different forms of scale-free activity, to determine if there are common or different mechanisms underlying each type of scaling behaviour.

One of the central challenges to the present work was to find a way to compare fundamentally different phenomena (cortical oscillations and scale-free activity) on the same scale with respect to their variability and task-responsiveness (our operational measures of stability/flexibility). This presents a number of challenges due to the differing characteristics of oscillatory and scale-free activity. Firstly, from the perspective of some researchers, cortical oscillations are a phenomenon which are dichotomous; they are either present or absent within an electrophysiological signal at a given time, while scale-free activity is always present (Kosciessa et al., 2020). This view presents a major challenge to comparing these metrics in terms of stability and flexibility: for example, does one consider variability of oscillatory power only when oscillations are present, or does one consider also their dwell-time? How does one account for task-evoked changes in power when an oscillation is present in one state but absent in another? Moreover, when taking this view it may not make sense to examine certain oscillations at all if there is not a corresponding peak in the power spectrum to indicate their significant presence.

In the present work, we take the view that cortical oscillations are always present, to greater or lesser degrees; the presence of an oscillatory peak merely indicates that a particular frequency has sufficient power at that point to be visible above the noise floor. In the supplementary materials, we present evidence that the dichotomous present/absent view of oscillations is inappropriate for our data (Supplementary Fig. S16). If the dichotomous view is to be applied to our analyses, there must be a clear boundary that can be established between the presence and absence of the oscillation; in other words, the distribution of power over time in a given frequency band should be bimodal. We observed no evidence of such bimodality in our data (Supplementary Fig. S16a). If such a boundary between oscillatory presence and absence is not easily defined, it renders the present analysis impossible, as raising or lowering the threshold for the presence of an oscillation will arbitrarily affect its variability (Supplementary Fig. S16b). Thus, while a complete discussion of whether cortical oscillations are binary or continuous phenomena is beyond the scope of this paper, we believe the view of oscillations as continuous phenomena is the most applicable for our present work.

Our choice of methods was likewise motivated by the above concerns. We chose to use the IRASA method, a resampling-based approach, to separate scale-free and oscillatory components of the power spectrum; however, newer methods have recently become available based on curve fitting which show promising results (Donoghue et al., 2020). While the advantages of the parametrization approach proposed by Donoghue et al. (2020) are well-argued, the FOOOF method proposed by Donoghue et al. (2020) requires the user to set the threshold for finding an oscillation: as discussed above, this is problematic for our analyses, as different parameter settings may predispose different variabilities for oscillatory processes. We further found that single-trial power spectra (in our time-locked analysis) were often too noisy to parametrize accurately with the method. As such, we chose to use the IRASA method with an extended range of resampling factors. While this approach is slightly less accurate than the FOOOF when a knee frequency is present, we believe this is necessary to ensure that our results do not depend on arbitrary parameter choices.

The second major consideration when comparing the variability of cortical oscillations and scale-free activity is the presence of unsystematic noise and its different expression within different frequency bands and metrics. For example, it is known that muscle artefacts have a frequency range of 20–300 Hz (Muthukumaraswamy, 2013), and environmental noise in an MEG scannel can take on a 1/f distribution (Mantini et al., 2011). The different influences of these noise components may have an influence on our comparative analysis of stability and flexibility: metrics which are affected by highly variable noise in-

fluences may appear more flexible, while metrics influenced by stable noise sources may appear more stable. While we cannot entirely rule out this concern, several aspects of our design limit its influence considerably. First, by operationalizing stability/flexibility in part by responsiveness to specific experimental stimuli (such as the HCP tasks and the CamCAN stimuli), we reduce the influence of noise components which do not vary systematically with experimental conditions. Secondly, we conducted a number of control analyses in the supplementary materials which attempt to take into account variations in unsystematic noise. In particular, we controlled for unsystematic noise by dividing the rest-task changes and inter-subject variability results by the level of spontaneous variation in resting-state (Supplementary Figs. S1–S6). Influences of noise on parameters' flexibility should be mostly captured by this within-subject variability; indeed, this is a conservative normalization, as spontaneous neural fluctuations in resting state are known to be behaviourally relevant for mind-wandering (Christoff et al., 2009), and thus likely vary between stable and flexible parameters as well. Despite this strict normalization procedure, the results of the main text generally held: the power-law exponent of scale-free activity remained one of the most stable parameters, while alpha power remained the most flexible. This suggests that while differences in the influence of noise components may be a source of error in our analysis, the main conclusions presented here are robust. Future work should consider other ways of controlling for unsystematic noise so as to be able to better compare the dynamics of scale-free and oscillatory processes.

Finally, due to the extreme computational intensiveness of the IRASA method, we were only able to assess time-resolved scale-free fluctuations in a subset of the original CamCAN data. Future work with greater computational resources should make an effort to investigate time-resolved fractal dynamics in larger samples and with multiple tasks, to begin to map out the task specificity (or un-specificity) of fractal responses to stimuli.

5. Conclusion

The brain must manage seemingly contradictory requirements in adapting to its environment: it must be flexible enough to adapt to incoming information, but at the same time maintain stability in response to noise. In the present work, we used MEG to investigate the stability and flexibility of different neural processes, namely fractal dynamics and cortical oscillations. Using novel analyses separating fractal and oscillatory components in resting state and various cognitive tasks and event-related designs, we demonstrate that fractal dynamics, in particular the power-law exponent, are stable in comparison with cortical oscillations; in particular, the PLE of scale-free activity showed the lowest variability and least responsiveness to external perturbations, while alpha-band oscillatory activity showed the greatest variability and task-responsiveness. Further, we demonstrate differences between the fractal PLE and broadband fractal power, with the latter being more flexible and task-responsive than the former. These results accord with theories of self-organized criticality in the brain, and suggest that the fractal PLE is a "background" parameter which may play a more facilitatory, predisposing, or enabling role in neural activity, rather than an active and causal one. Finally, the results raise intriguing questions regarding the importance of scale-free activity to the brain by suggesting that the power-law exponent may function as a regulated variable maintained in a stable manner near a physiological set point.

Data and code availability

Data from the Human Connectome Project can be accessed at https://db.humanconnectome.org/. Data from the Cambridge Center for Aging Neuroscience project can be accessed at https://camcan-archive.mrc-cbu.cam.ac.uk/dataaccess/. Code for this project is freely available at https://github.com/SorenWT/oscifrac2021.

Ethics statement

Data collection for the CamCAN dataset was approved by the Cambridgeshire 2 Research Ethics Committee (reference: 10/H0308/50). This project was approved by the Institutional Review Board of the University of Ottawa's Institute of Mental Health Research (approval #2021002).

Declaration of Competing Interest

The authors declare no competing interests.

Credit authorship contribution statement

Soren Wainio-Theberge: Visualization, Formal analysis, Methodology, Writing – original draft. **Annemarie Wolff:** Writing – review & editing. **Javier Gomez-Pilar:** Writing – review & editing. **Jianfeng Zhang:** Writing – review & editing. **Georg Northoff:** Visualization, Writing – original draft.

Acknowledgments

GN has received funding from the European Union's Horizon 2020 Framework Programme for Research and Innovation under the Specific Grant Agreement No. 785907 (Human Brain Project SGA2). GN is grateful for funding provided by UMRF, uOBMRI, CIHR (201103MOP-244752-BSBCECA-179644; 201103CCI-248496-CCI-CECA), the Canada-UK Artificial Intelligence Initiative (ES/T01279X/1), and PSI. JGP acknowledges funding from 'CIBER in Bioengineering, Biomaterials and Nanomedicine (CIBER-BBN)' through 'Instituto de Salud Carlos III', co-funded with FEDER funds. Data were provided (in part) by the Human Connectome Project, WU-Minn Consortium (Principal Investigators: David Van Essen and Kamil Ugurbil; 1U54MH091657) funded by the 16 NIH Institutes and Centers that support the NIH Blueprint for Neuroscience Research; and by the McDonnell Center for Systems Neuroscience at Washington University. Data collection and sharing for this project was provided (in part) by the Cambridge Centre for Ageing and Neuroscience (CamCAN). CamCAN funding was provided by the UK Biotechnology and Biological Sciences Research Council (grant number BB/H008217/1), together with support from the UK Medical Research Council and University of Cambridge, UK.

Supplementary materials

Supplementary material associated with this article can be found, in the online version, at doi:10.1016/j.neuroimage.2022.119245.

References

Ahlfors, S.P., Han, J., Belliveau, J.W., Hämäläinen, M.S., 2010. Sensitivity of MEG and EEG to source orientation. Brain Topogr. 23, 227–232. doi:10.1007/s10548-010-0154-x.

Armbruster-Genç, D.J.N., Ueltzhöffer, K., Fiebach, C.J., 2016. Brain signal variability differentially affects cognitive flexibility and cognitive stability. J. Neurosci. 36, 3978–3987. doi:10.1523/JNEUROSCI.2517-14.2016.

Bai, Y., Nakao, T., Xu, J., Qin, P., Chaves, P., Heinzel, A., Duncan, N., Lane, T., Yen, N.S., Tsai, S.Y., Northoff, G., 2016. Resting state glutamate predicts elevated pre-stimulus alpha during self-relatedness: a combined EEG-MRS study on "rest-self overlap. Soc. Neurosci. 11, 249–263. doi:10.1080/17470919.2015.1072582.

Beggs, J.M., 2008. The criticality hypothesis: how local cortical networks might optimize information processing. Philos. Trans. R. Soc. Math. Phys. Eng. Sci. 366, 329–343. doi:10.1098/rsta.2007.2092.

Benjamini, Y., Yekutieli, D., 2001. The control of the false discovery rate in multiple testing under dependency. Ann. Stat. 29, 1165–1188. doi:10.1214/aos/1013699998.

Buzsáki, G., 2006. Rhythms of the Brain, Rhythms of the Brain. Oxford University Press, New York, NY, US doi:10.1093/acprof:oso/9780195301069.001.0001.

Chaplin, W.F., John, O.P., Goldberg, L.R., 1988. Conceptions of states and traits: dimensional attributes with ideals as prototypes. J. Personal. Soc. Psychol. 54, 541–557. doi:10.1037//0022-3514.54.4.541.

Chialvo, D.R., 2010. Emergent complex neural dynamics. Nat. Phys. 6, 744–750.

Christoff, K., Gordon, A.M., Smallwood, J., Smith, R., Schooler, J.W., 2009. Experience sampling during fMRI reveals default network and executive system contributions to mind wandering. Proc. Natl. Acad. Sci. 106, 8719–8724. doi:10.1073/pnas.0900234106.

Cocchi, L., Gollo, L.L., Zalesky, A., Breakspear, M., 2017. Criticality in the brain: a synthesis of neurobiology, models and cognition. Prog. Neurobiol. 158, 132–152. doi:10.1016/j.pneurobio.2017.07.002.

Cohen, M.X., 2014. Fluctuations in oscillation frequency control spike timing and coordinate neural networks. J. Neurosci. 34, 8988–8998. doi:10.1523/JNEUROSCI.0261-14.2014.

Cools, R., 2019. Chemistry of the adaptive mind: lessons from dopamine. Neuron 104, 113–131. doi:10.1016/j.neuron.2019.09.035.

Dajani, D.R., Uddin, L.Q., 2015. Demystifying cognitive flexibility: implications for clinical and developmental neuroscience. Trends Neurosci. 38, 571–578. doi:10.1016/j.tins.2015.07.003.

Dale, A.M., Fischl, B., Sereno, M.I., 1999. Cortical surface-based analysis: I. Segmentation and surface reconstruction. Neuroimage 9, 179–194.

Dave, S., Brothers, T.A., Swaab, T.Y., 2018. 1/f neural noise and electrophysiological indices of contextual prediction in aging. Brain Res. 1691, 34–43. doi:10.1016/j.brainres.2018.04.007.

Delorme, A., Makeig, S., 2004. EEGLAB: an open source toolbox for analysis of single-trial EEG dynamics including independent component analysis. J. Neurosci. Methods 134, 9–21. doi:10.1016/j.jneumeth.2003.10.009.

Donoghue, T., Haller, M., Peterson, E.J., Varma, P., Sebastian, P., Gao, R., Noto, T., Lara, A.H., Wallis, J.D., Knight, R.T., Shestyuk, A., Voytek, B., 2020. Parameterizing neural power spectra into periodic and aperiodic components. Nat. Neurosci. 23, 1655–1665. doi:10.1038/s41593-020-00744-x.

Dreisbach, G., Müller, J., Goschke, T., Strobel, A., Schulze, K., Lesch, K.P., Brocke, B., 2005. Dopamine and cognitive control: the influence of spontaneous eyeblink rate and dopamine gene polymorphisms on perseveration and distractibility. Behav. Neurosci. 119, 483.

Durstewitz, D., Seamans, J.K., 2008. The dual-state theory of prefrontal cortex dopamine function with relevance to catechol-O-methyltransferase genotypes and schizophrenia. Biol. Psychiatry 64, 739–749. doi:10.1016/j.biopsych.2008.05.015, Neurodevelopment and the Transition from Schizophrenia Prodrome to Schizophrenia.

Eke, A., Herman, P., Kocsis, L., Kozak, L.R., 2002. Fractal characterization of complexity in temporal physiological signals. Physiol. Meas. 23, R1–R38. doi:10.1088/0967-3334/23/1/201.

Ferri, F., Nikolova, Y.S., Perrucci, M.G., Costantini, M., Ferretti, A., Gatta, V., Huang, Z., Edden, R.A.E., Yue, Q., D'Aurora, M., Sibille, E., Stuppia, L., Romani, G.L., Northoff, G., 2017. A neural "Tuning Curve" for multisensory experience and cognitive-perceptual schizotypy. Schizophr. Bull. 43, 801–813. doi:10.1093/schbul/sbw174.

Fodor, Z., Marosi, C., Tombor, L., Csukly, G., 2020. Salient distractors open the door of perception: alpha desynchronization marks sensory gating in a working memory task. Sci. Rep. 10, 19179. doi:10.1038/s41598-020-76190-3.

Fossion, R., Fossion, J.P.J., Rivera, A.L., Lecona, O.A., Toledo-Roy, J.C., García-Pelagio, K.P., García-Iglesias, L., Estañol, B., Olivares-Quiroz, L., Resendis-Antonio, O., 2018a. Homeostasis from a time-series perspective: an intuitive interpretation of the variability of physiological variables. In: Quantitative Models for Microscopic to Macroscopic Biological Macromolecules and Tissues. Springer International Publishing, Cham, pp. 87–109. doi:10.1007/978-3-319-73975-5_5.

Fossion, R., Rivera, A.L., Estañol, B., 2018b. A physicist's view of homeostasis: how time series of continuous monitoring reflect the function of physiological variables in regulatory mechanisms. Physiol. Meas. 39, 084007. doi:10.1088/1361-6579/aad8db.

Foxe, J.J., Snyder, A.C., 2011. The role of alpha-band brain oscillations as a sensory suppression mechanism during selective attention. Front. Psychol. 2. doi:10.3389/fpsyg.2011.00154.

Friston, K.J., Rosch, R., Parr, T., Price, C., Bowman, H., 2018. Deep temporal models and active inference. Neurosci. Biobehav. Rev. 90, 486–501. doi:10.1016/j.neubiorev.2018.04.004.

Fujino, J., Tei, S., Jankowski, K.F., Kawada, R., Murai, T., Takahashi, H., 2017. Role of spontaneous brain activity in explicit and implicit aspects of cognitive flexibility under socially conflicting situations: a resting-state fmri study using fractional amplitude of low-frequency fluctuations. Neuroscience 367, 60–71. doi:10.1016/j.neuroscience.2017.10.025.

Garrett, D.D., Kovacevic, N., McIntosh, A.R., Grady, C.L., 2011. The importance of being variable. J. Neurosci. Off. J. Soc. Neurosci. 31, 4496–4503. doi:10.1523/JNEUROSCI.5641-10.2011.

Garrett, D.D., Samanez-Larkin, G.R., MacDonald, S.W.S., Lindenberger, U., McIntosh, A.R., Grady, C.L., 2013. Moment-to-moment brain signal variability: a next frontier in human brain mapping? Neurosci. Biobehav. Rev. 37, 610–624. doi:10.1016/j.neubiorev.2013.02.015.

Glasser, M.F., Coalson, T.S., Robinson, E.C., Hacker, C.D., Harwell, J., Yacoub, E., Ugurbil, K., Andersson, J., Beckmann, C.F., Jenkinson, M., Smith, S.M., Van Essen, D.C., 2016. A multi-modal parcellation of human cerebral cortex. Nature 536, 171–178. doi:10.1038/nature18933.

Golesorkhi, M., Gomez-Pilar, J., Tumati, S., Fraser, M., Northoff, G., 2021. Temporal hierarchy of intrinsic neural timescales converges with spatial core-periphery organization. Commun. Biol. 4, 1–14. doi:10.1038/s42003-021-01785-z.

Goschke, T., 2003. Voluntary action and cognitive control from a cognitive neuroscience perspective. In: Voluntary Action: Brains, Minds, and Sociality. Oxford University Press, New York, NY, US, pp. 49–85.

Güntekin, B., Başar, E., 2016. Review of evoked and event-related delta responses in the human brain. Int. J. Psychophysiol. 103, 43–52. doi:10.1016/j.ijpsycho.2015.02.001, Res. Brain Oscillations and Connectivity in A New Take-Off State.

Halder, T., Talwar, S., Jaiswal, A.K., Banerjee, A., 2019. Quantitative evaluation in estimating sources underlying brain oscillations using current source density methods and beamformer approaches. eNeuro 6. doi:10.1523/ENEURO.0170-19.2019.

He, B.J., 2014. Scale-free brain activity: past, present, and future. Trends Cogn. Sci. 18, 480–487. doi:10.1016/j.tics.2014.04.003.

He, B.J., Zempel, J.M., Snyder, A.Z., Raichle, M.E., 2010. The temporal structures and functional significance of scale-free brain activity. Neuron 66, 353–369. doi:10.1016/j.neuron.2010.04.020.

Herweg, N.A., Solomon, E.A., Kahana, M.J., 2020. Theta oscillations in human memory. Trends Cogn. Sci. 24, 208–227. doi:10.1016/j.tics.2019.12.006.

Hesse, J., Gross, T., 2014. Self-organized criticality as a fundamental property of neural systems. Front. Syst. Neurosci. 8. doi:10.3389/fnsys.2014.00166.

Holm, S., 1979. A simple sequentially rejective multiple test procedure. Scand. J. Stat. 6, 65–70.

Huang, Z., Obara, N., Davis, H.H., Pokorny, J., Northoff, G., 2016. The temporal structure of resting-state brain activity in the medial prefrontal cortex predicts self-consciousness. Neuropsychologia 82, 161–170. doi:10.1016/j.neuropsychologia.2016.01.025.

Huang, Z., Zhang, J., Longtin, A., Dumont, G., Duncan, N.W., Pokorny, J., Qin, P., Dai, R., Ferri, F., Weng, X., Northoff, G., 2017. Is there a nonadditive interaction between spontaneous and evoked activity? Phase-dependence and its relation to the temporal structure of scale-free brain activity. Cereb. Cortex 27, 1037–1059. doi:10.1093/cercor/bhv288, N. Y. N 1991.

Ito, T., Hearne, L.J., Cole, M.W., 2020. A cortical hierarchy of localized and distributed processes revealed via dissociation of task activations, connectivity changes, and intrinsic timescales. Neuroimage 221, 117141. doi:10.1016/j.neuroimage.2020.117141.

Jas, M., Engemann, D.A., Bekhti, Y., Raimondo, F., Gramfort, A., 2017. Autoreject: Automated artifact rejection for MEG and EEG data. Neuroimage 159, 417–429. doi:10.1016/j.neuroimage.2017.06.030.

Jenkinson, N., Brown, P., 2011. New insights into the relationship between dopamine, beta oscillations and motor function. Trends Neurosci. 34, 611–618. doi:10.1016/j.tins.2011.09.003.

Kasagi, M., Huang, Z., Narita, K., Shitara, H., Motegi, T., Suzuki, Y., Fujihara, K., Tanabe, S., Kosaka, H., Ujita, K., Fukuda, M., Northoff, G., 2017. Association between scale-free brain dynamics and behavioral performance: functional MRI study in resting state and face processing task. Behav. Neurol. 2017, 2824615. doi:10.1155/2017/2824615.

Kim, M., Lee, U., 2019. Alpha oscillation, criticality, and responsiveness in complex brain networks. Netw. Neurosci. 4, 155–173. doi:10.1162/netn_a_00113.

Klimesch, W., 2012. α-band oscillations, attention, and controlled access to stored information. Trends Cogn. Sci. 16, 606–617. doi:10.1016/j.tics.2012.10.007.

Klimesch, W., 1999. EEG alpha and theta oscillations reflect cognitive and memory performance: a review and analysis. Brain Res. Brain Res. Rev. 29, 169–195.

Klimesch, W., Doppelmayr, M., Hanslmayr, S., Neuper, C., Klimesch, W., 2006. Upper alpha ERD and absolute power: their meaning for memory performance. In: Progress in Brain Research, Event-Related Dynamics of Brain Oscillations. Elsevier, pp. 151–165. doi:10.1016/S0079-6123(06)59010-7.

Knyazev, G.G., 2007. Motivation, emotion, and their inhibitory control mirrored in brain oscillations. Neurosci. Biobehav. Rev. 31, 377–395. doi:10.1016/j.neubiorev.2006.10.004.

Knyazev, G.G., Savostyanov, A.N., Levin, E.A., 2004. Alpha oscillations as a correlate of trait anxiety. Int. J. Psychophysiol. 53, 147–160. doi:10.1016/j.ijpsycho.2004.03.001.

Kolvoort, I.R., Wainio-Theberge, S., Wolff, A., Northoff, G., 2020. Temporal integration as "common currency" of brain and self-scale-free activity in resting-state EEG correlates with temporal delay effects on self-relatedness. Hum. Brain Mapp. 41, 4355–4374. doi:10.1002/hbm.25129.

Koopmans, L.H., Owen, D.B., Rosenblatt, J.I., 1964. Confidence intervals for the coefficient of variation for the normal and log normal distributions. Biometrika 51, 25–32. doi:10.1093/biomet/51.1-2.25.

Kosciessa, J.Q., Grandy, T.H., Garrett, D.D., Werkle-Bergner, M., 2020. Single-trial characterization of neural rhythms: Potential and challenges. Neuroimage 206, 116331. doi:10.1016/j.neuroimage.2019.116331.

Kounios, J., Fleck, J.I., Green, D.L., Payne, L., Stevenson, J.L., Bowden, E.M., Jung-Beeman, M., 2008. The origins of insight in resting-state brain activity. Neuropsychologia 46, 281–291. doi:10.1016/j.neuropsychologia.2007.07.013.

Larson-Prior, L.J., Oostenveld, R., Della Penna, S., Michalareas, G., Prior, F., Babajani-Feremi, A., Schoffelen, J.M., Marzetti, L., de Pasquale, F., Di Pompeo, F., Stout, J., Woolrich, M., Luo, Q., Bucholz, R., Fries, P., Pizzella, V., Romani, G.L., Corbetta, M., Snyder, A.Z., 2013. Adding dynamics to the human connectome project with MEG. NeuroImage, Mapp. Connect. 80, 190–201. doi:10.1016/j.neuroimage.2013.05.056.

Linkenkaer-Hansen, K., Nikouline, V.V., Palva, J.M., Ilmoniemi, R.J., 2001. Long-range temporal correlations and scaling behavior in human brain oscillations. J. Neurosci. Off. J. Soc. Neurosci. 21, 1370–1377.

Lombardi, F., Herrmann, H.J., de Arcangelis, L., 2017. Balance of excitation and inhibition determines 1/f power spectrum in neuronal networks. Chaos Interdiscip. J. Nonlinear Sci. 27, 047402. doi:10.1063/1.4979043.

Lombardi, F., Herrmann, H.J., Perrone-Capano, C., Plenz, D., de Arcangelis, L., 2012. Balance between excitation and inhibition controls the temporal organization of neuronal avalanches. Phys. Rev. Lett. 108, 228703. doi:10.1103/PhysRevLett.108.228703.

Luck, S.J., 2014. An Introduction to the Event-Related Potential Technique. MIT press.

MacLean, M.H., Arnell, K.M., Cote, K.A., 2012. Resting EEG in alpha and beta bands predicts individual differences in attentional blink magnitude. Brain Cogn. 78, 218–229. doi:10.1016/j.bandc.2011.12.010.

Maguire, M.J., Brier, M.R., Ferree, T.C., 2010. EEG theta and alpha responses reveal qualitative differences in processing taxonomic versus thematic semantic relationships. Brain Lang. 114, 16–25. doi:10.1016/j.bandl.2010.03.005.

Makeig, S., 1993. Auditory event-related dynamics of the EEG spectrum and effects of exposure to tones. Electroencephalogr. Clin. Neurophysiol. 86, 283–293. doi:10.1016/0013-4694(93)90110-H.

Mantini, D., Penna, S.D., Marzetti, L., de Pasquale, F., Pizzella, V., Corbetta, M., Romani, G.L., 2011. A signal-processing pipeline for magnetoencephalography resting-state networks. Brain Connect. 1, 49–59. doi:10.1089/brain.2011.0001.

Maris, E., Oostenveld, R., 2007. Nonparametric statistical testing of EEG- and MEG-data. J. Neurosci. Methods 164, 177–190. doi:10.1016/j.jneumeth.2007.03.024.

McCutcheon, R.A., Krystal, J.H., Howes, O.D., 2020. Dopamine and glutamate in schizophrenia: biology, symptoms and treatment. World Psychiatry 19, 15–33. doi:10.1002/wps.20693.

Modell, H., Cliff, W., Michael, J., McFarland, J., Wenderoth, M.P., Wright, A., 2015. A physiologist's view of homeostasis. Adv. Physiol. Educ. 39, 259–266. doi:10.1152/advan.00107.2015.

Muthukumaraswamy, S.D., 2013. High-frequency brain activity and muscle artifacts in MEG/EEG: a review and recommendations. Front. Hum. Neurosci. 7, 138. doi:10.3389/fnhum.2013.00138.

Muthukumaraswamy, S.D., Liley, D.T.J., 2018. 1/f electrophysiological spectra in resting and drug-induced states can be explained by the dynamics of multiple oscillatory relaxation processes. Neuroimage 179, 582–595. doi:10.1016/j.neuroimage.2018.06.068.

Nomi, J.S., Bolt, T.S., Ezie, C.E.C., Uddin, L.Q., Heller, A.S., 2017. Moment-to-moment BOLD signal variability reflects regional changes in neural flexibility across the lifespan. J. Neurosci. 37, 5539–5548. doi:10.1523/JNEUROSCI.3408-16.2017.

Northoff, G., 2017. Personal identity and cortical midline structure (CMS): do temporal features of CMS neural activity transform into "Self-Continuity"? Psychol. Inq. 28, 122–131.

Northoff, G., 2013. Unlocking the Brain: Volume 2: Consciousness. Unlocking the Brain: Volume 2: Consciousness. Oxford University Press.

Northoff, G., Heiss, W.D., 2015. Why is the distinction between neural predispositions, prerequisites, and correlates of the level of consciousness clinically relevant? Functional brain imaging in coma and vegetative state. Stroke 46, 1147–1151.

Northoff, G., Lamme, V., 2020. Neural signs and mechanisms of consciousness: is there a potential convergence of theories of consciousness in sight? Neurosci. Biobehav. Rev. doi:10.1016/j.neubiorev.2020.07.019.

Northoff, G., Sandsten, K.E., Nordgaard, J., Kjaer, T.W., Parnas, J., 2020. The self and its prolonged intrinsic neural timescale in schizophrenia. Schizophr. Bull. doi:10.1093/schbul/sbaa083.

Oostenveld, R., Fries, P., Maris, E., Schoffelen, J.M., 2011. FieldTrip: open source software for advanced analysis of MEG, EEG, and invasive electrophysiological data [WWW Document]. Comput. Intell. Neurosci. doi:10.1155/2011/156869.

Ouyang, G., Hildebrandt, A., Schmitz, F., Herrmann, C.S., 2020. Decomposing alpha and 1/f brain activities reveals their differential associations with cognitive processing speed. Neuroimage 205, 116304. doi:10.1016/j.neuroimage.2019.116304.

Palva, J.M., Zhigalov, A., Hirvonen, J., Korhonen, O., Linkenkaer-Hansen, K., Palva, S., 2013. Neuronal long-range temporal correlations and avalanche dynamics are correlated with behavioral scaling laws. Proc. Natl. Acad. Sci. 110, 3585–3590. doi:10.1073/pnas.1216855110.

Palva, S., Palva, J.M., 2007. New vistas for α-frequency band oscillations. Trends Neurosci. 30, 150–158. doi:10.1016/j.tins.2007.02.001.

Pascual-Marqui, R.D., Faber, P., Kinoshita, T., Kochi, K., Milz, P., Nishida, K., Yoshimura, M., 2018. Comparing EEG/MEG neuroimaging methods based on localization error, false positive activity, and false positive connectivity. bioRxiv 269753. doi:10.1101/269753.

Pascual-Marqui, R.D., Lehmann, D., Koukkou, M., Kochi, K., Anderer, P., Saletu, B., Tanaka, H., Hirata, K., John, E.R., Prichep, L., Biscay-Lirio, R., Kinoshita, T., 2011. Assessing interactions in the brain with exact low-resolution electromagnetic tomography. Philos. Trans. R. Soc. Math. Phys. Eng. Sci. 369, 3768–3784. doi:10.1098/rsta.2011.0081.

Penn, A.C., 2020. iboot: Iterated bootstrap for small samples or samples with complex dependence structures [https://github.com/acp29/iboot]. Zenodo. https://doi.org/10.5281/zenodo.6326873.

Pfurtscheller, G., Lopes da Silva, F.H., 1999. Event-related EEG/MEG synchronization and desynchronization: basic principles. Clin. Neurophysiol. Off. J. Int. Fed. Clin. Neurophysiol. 110, 1842–1857. doi:10.1016/s1388-2457(99)00141-8.

Pitchford, B., Arnell, K.M., 2019. Resting EEG in alpha and beta bands predicts individual differences in attentional breadth. Conscious Cogn. 75, 102803. doi:10.1016/j.concog.2019.102803.

Poil, S.S., Hardstone, R., Mansvelder, H.D., Linkenkaer-Hansen, K., 2012. Critical-state dynamics of avalanches and oscillations jointly emerge from balanced excitation/inhibition in neuronal networks. J. Neurosci. 32, 9817–9823. doi:10.1523/JNEUROSCI.5990-11.2012.

Racz, F.S., Stylianou, O., Mukli, P., Eke, A., 2019. Multifractal and entropy analysis of resting-state electroencephalography reveals spatial organization in local dynamic functional connectivity. Sci. Rep. 9, 13474. doi:10.1038/s41598-019-49726-5.

Raut, R.V., Mitra, A., Marek, S., Ortega, M., Snyder, A.Z., Tanenbaum, A., Laumann, T.O., Dosenbach, N.U.F., Raichle, M.E., 2020. Organization of propagated intrinsic brain activity in individual humans. Cereb. Cortex 30, 1716–1734. doi:10.1093/cercor/bhz198.

Riedel, P., Domachowska, I.M., Lee, Y., Neukam, P.T., Tönges, L., Li, S.C., Goschke, T., Smolka, M.N., 2022. L-DOPA administration shifts the stability-flexibility balance towards attentional capture by distractors during a visual search task. Psychopharmacology doi:10.1007/s00213-022-06077-w, (Berl.).

Scalabrini, A., Ebisch, S.J.H., Huang, Z., Di Plinio, S., Perrucci, M.G., Romani, G.L., Mucci, C., Northoff, G., 2019. Spontaneous brain activity predicts task-evoked activity during animate versus inanimate touch. Cereb. Cortex 1991. doi:10.1093/cercor/bhy340, N. Y. N.

Shafto, M.A., Tyler, L.K., Dixon, M., Taylor, J.R., Rowe, J.B., Cusack, R., Calder, A.J., Marslen-Wilson, W.D., Duncan, J., Dalgleish, T., Henson, R.N., Brayne, C., Matthews, F.E.Cam-CAN, 2014. The Cambridge centre for ageing and neuroscience (cam-CAN) study protocol: a cross-sectional, lifespan, multidisciplinary examination of healthy cognitive ageing. BMC Neurol. 14, 204. doi:10.1186/s12883-014-0204-1.

Steyer, R., Mayer, A., Geiser, C., Cole, D.A., 2015. A theory of states and traits—revised. Annu. Rev. Clin. Psychol. 11, 71–98. doi:10.1146/annurev-clinpsy-032813-153719.

Sun, J., Tang, Y., Lim, K.O., Wang, J., Tong, S., Li, H., He, B., 2014. Abnormal dynamics of EEG oscillations in schizophrenia patients on multiple time scales. IEEE Trans. Biomed. Eng. 61, 1756–1764. doi:10.1109/TBME.2014.2306424.

Tagliazucchi, E., Chialvo, D.R., Siniatchkin, M., Amico, E., Brichant, J.F., Bonhomme, V., Noirhomme, Q., Laufs, H., Laureys, S., 2016. Large-scale signatures of unconsciousness are consistent with a departure from critical dynamics. J. R. Soc. Interface 13, 20151027. doi:10.1098/rsif.2015.1027.

Tagliazucchi, E., von Wegner, F., Morzelewski, A., Brodbeck, V., Jahnke, K., Laufs, H., 2013. Breakdown of long-range temporal dependence in default mode and attention networks during deep sleep. Proc. Natl. Acad. Sci. U. S. A. 110, 15419–15424. doi:10.1073/pnas.1312848110.

Taylor, J.R., Williams, N., Cusack, R., Auer, T., Shafto, M.A., Dixon, M., Tyler, L.K., Henson, R.N.Cam-CAN, 2017. The cambridge centre for ageing and neuroscience (Cam-CAN) data repository: structural and functional MRI, MEG, and cognitive data from a cross-sectional adult lifespan sample. NeuroImage 144, 262–269. doi:10.1016/j.neuroimage.2015.09.018, Data Sharing Part II.

Van Essen, D.C., Glasser, M.F., Dierker, D.L., Harwell, J., Coalson, T., 2012. Parcellations and hemispheric asymmetries of human cerebral cortex analyzed on surface-based atlases. Cereb. Cortex 22, 2241–2262. doi:10.1093/cercor/bhr291.

Voytek, B., Kramer, M.A., Case, J., Lepage, K.Q., Tempesta, Z.R., Knight, R.T., Gazzaley, A., 2015. Age-related changes in 1/f neural electrophysiological noise. J. Neurosci. 35, 13257–13265. doi:10.1523/JNEUROSCI.2332-14.2015.

Wainio-Theberge, S., Wolff, A., Northoff, G., 2020. Bridging the gap – spontaneous fluctuations shape stimulus-evoked spectral power. bioRxiv doi:10.1101/2020.06.23.166058.

Waschke, L., Kloosterman, N.A., Obleser, J., Garrett, D.D., 2021. Behavior needs neural variability. Neuron doi:10.1016/j.neuron.2021.01.023.

Waschke, L., Wöstmann, M., Obleser, J., 2017. States and traits of neural irregularity in the age-varying human brain. Sci. Rep. 7, 17381. doi:10.1038/s41598-017-17766-4.

Wen, H., Liu, Z., 2016a. Broadband electrophysiological dynamics contribute to global resting-state fMRI signal. J. Neurosci. 36, 6030–6040. doi:10.1523/JNEUROSCI.0187-16.2016.

Wen, H., Liu, Z., 2016b. Separating fractal and oscillatory components in the power spectrum of neurophysiological signal. Brain Topogr. 29, 13–26. doi:10.1007/s10548-015-0448-0.

Williams, S., Boksa, P., 2010. Gamma oscillations and schizophrenia. J. Psychiatry Neurosci. JPN 35, 75–77. doi:10.1503/jpn.100021.

Wolff, A., Di Giovanni, D.A., Gómez-Pilar, J., Nakao, T., Huang, Z., Longtin, A., Northoff, G., 2018. The temporal signature of self: temporal measures of resting-state EEG predict self-consciousness. Hum. Brain Mapp 40, 789–803. doi:10.1002/hbm.24412.

Wolff, A., Yao, L., Gomez-Pilar, J., Shoaran, M., Jiang, N., Northoff, G., 2019. Neural variability quenching during decision-making: neural individuality and its prestimulus complexity. Neuroimage 192, 1–14. doi:10.1016/j.neuroimage.2019.02.070.

Zhang, J., Huang, Z., Chen, Y., Zhang, J., Ghinda, D., Nikolova, Y., Wu, J., Xu, J., Bai, W., Mao, Y., Yang, Z., Duncan, N., Qin, P., Wang, H., Chen, B., Weng, X., Northoff, G., 2018. Breakdown in the temporal and spatial organization of spontaneous brain activity during general anesthesia. Hum. Brain Mapp. 39, 2035–2046. doi:10.1002/hbm.23984.

Zilio, F., Gomez-Pilar, J., Cao, S., Zhang, J., Zang, D., Qi, Z., Tan, J., Hiromi, T., Wu, X., Fogel, S., Huang, Z., Hohmann, M.R., Fomina, T., Synofzik, M., Grosse-Wentrup, M., Owen, A.M., Northoff, G., 2020. Intrinsic neural timescales related to sensory processing: Evidence from abnormal behavioural states. bioRxiv doi:10.1101/2020.07.30.229161, 2020.07.30.229161.